

ESTIMATING STATE OF CHARGE OF SMALL SCALE BATTERY STORAGE

LIBRARY
UNIVERSITY OF MORATUWA, SRI LANKA
MORATUWA

Nisal Dininda Amarasinghe

(119118B)

Thesis/Dissertation submitted in partial fulfillment of the requirements for the degree
Master of Science of Electrical Installation.

Department of Electrical Engineering

University of Moratuwa

Sri Lanka

August 2016

University of Moratuwa



TH3227

621.3¹⁶
696.6 (0+3)

TH3227

+ CD-ROM

TH3227

DECLARATION

“I declare that this is my own work and this dissertation does not incorporate without acknowledgement any material previously submitted for a Degree or Diploma in any other University or institute of higher learning and to the best of my knowledge and belief it does not contain any material previously published or written by another person except where the acknowledgement is made in the text.

Also, I hereby grant to University of Moratuwa the non-exclusive right to reproduce and distribute my dissertation, in whole or in part in print, electronic or other medium. I retain the right to use this content in whole or part in future works (such as articles or books)”.



University of Moratuwa, Sri Lanka.
Electronic Theses & Dissertations
www.lib.mrt.ac.lk

Signature of the candidate

Date:

(N.D.Amarasinghe)

The above candidate has carried out research for the Masters Dissertation under my supervision.

.....

Signature of the supervisor

Date:

(Prof. Sisil Kumarawadu)

ABSTRACT

Lead-acid batteries are often used as the energy storage component for small-scale photo-voltaic(PV), systems in the developing world, allowing electricity to be supplied when generation is not occurring. Batteries often account for a significant fraction of the capital cost of the system and also have the shortest lifetime when compared to solar panels ect. In simple systems, the management of the battery sub-system is often crude, with the battery charged directly via a solar panel through a simple reverse-blocking diode and supplying an inverter incorporating a simple under-voltage cut-out in an attempt to avoid over-discharge. This leads to frequent over-charging (and over-discharging if the voltage cut-out is set incorrectly) of batteries and early failure, necessitating costly refurbishment or replacement. Also when several batteries are in series or parallel the extractable energy from the whole battery is limited by the capability of the weakest battery in the group. But if the SOC(State of Charge) batteries in a group, can be determined in advance, to determine the point of cut-off for charging or discharging, the extractable energy can be increased without sacrificing the life of batteries. This paper discuss different techniques that are used today in determining the SOC of batteries in the lines of its applicability of the particular case of group of batteries. This thesis thoroughly investigate the applicability of state variable approach proposed by John Chiasson and Baskar Vairamohan in “Estimating the State of Charge of a Battery” for the case of more than one battery, where it considers only terminal voltage and current of the battery for estimating the SOC. In this approach a non-linear time varying system is simplified to a linear time varying system with some reasonable assumptions. This approach was verified for different types of batteries at different state of health. It was also verified that the same method is applicable to find out the week battery in a string of series of batteries. The paper in its final chapter proposes a technique which is general and applicable for determining the discharge cut-off point based on rate of change of terminal voltage.

Key words: State of charge, Control theory, Battery.

ACKNOWLEDGEMENT

First, I pay my sincere gratitude to Prof. Sisil Kumarawadu who encouraged and guided me to conduct this investigation and on preparation of final dissertation.

I also take this opportunity to thank to Eng. Anuruddha Madawala who gave me tremendous support in facilitating testing equipment and instruments for simulations. And also for the encouragement and support in preparation of final dissertation.

It is a great pleasure to remember the kind co-operation and encouragement extended by my wife Madhushani Buddhadasa who helped me to continue the studies from start to end.



University of Moratuwa, Sri Lanka.
Electronic Theses & Dissertations
www.lib.mrt.ac.lk

Contents

CHAPTER 1	1
Introduction.....	1
1.1 Background	1
1.2 Identification of the Problem & Motivation.....	2
1.3 Objective of the Study.....	5
1.4 Methodology	5
CHAPTER 2	6
Lead acid battery characteristics.	6
2.1 Aging of battery.	6
2.2 Battery depth of discharge Vs cycle life.	6
2.3 Battery charging	7
2.4 Main power (Cycle use).....	7
2.4.1 Constant voltage charging method.....	7
2.4.2 Constant voltage – constant current charging method	8
2.5 Standby / Back up use charging	9
2.5.1 Trickle charge system.	9
2.5.2 Float charge system.....	10
2.6 Self discharge and refresh charge.	10
2.7 Charging voltage and the ambient temperature.	11
2.8 Discharging of a lead acid battery.....	12
2.9 Open circuit voltage of a battery.....	12
2.10 Open circuit voltage of a battery stabilization time.	14
2.11 Relationship between open circuit voltage (OCV) and state of charge(SOC). ...	14
2.12 Coup de fouet region.....	14
2.13 Overcharging.....	17

2.14	Undercharging.....	17
2.15	Discharge rate Vs Extractable energy	17
Chapter 3.....		19
Battery state of charge estimation techniques.....		19
3.1	Open circuit discharge test.....	19
3.2	Coulomb counting method.....	20
3.3	Peukerts equation based method.....	21
3.4	Observation and behavioral methods.....	23
3.5	Battery electrical models.....	23
Chapter 4.....		26
Battery Test setup		26
4.1	Development of hardware in the loop (HIL) simulation test setup.....	26
4.2	Voltage and current measurement.....	28
4.3	Charge source- programmable remote controllable power supply(PSI8080)	30
4.4	Electronic load- Programmable remote controllable electronic load(EL975)	30
4.5	Protection of the system.....	31
4.6	Simulink program.....	31
4.7	Load profile setter sub system.....	32
4.7.1	Communication with Electronic Load and Power Supply.....	34
4.7.2	Clock1	35
4.7.3	Clock2.....	35
4.7.4	Pulse generator.....	35
4.7.5	Current profile(i).....	35
4.7.6	Set voltage.....	35
The appropriate voltage at which the batteries should be charged.....		35
4.7.7	Current sensor resistance.....	36

This is the actual resistance of current sensing resistor.....	36
4.7.8 Voltage divider ratio.....	36
4.7.9 V_cut_off.....	36
4.7.10 I_cut_of.....	37
4.7.11 Cycles.....	37
4.7.12 Soft Real Time.....	37
4.8 PICO measurements sub system.....	37
4.8.1 Communication with ADC-20 Data logger.....	38
4.8 Standard charge – discharge monitor setup with HIOKI recorder.....	41
Chapter 5.....	42
Modified Thevenin's model based estimation of SOC.....	42
5.1 Basic equations for discharging.....	43
By applying Kirchhoff's Current Law, considering discharging case.....	43
5.2 Construct State Space model.....	43
5.3 Identify the final objective.....	44
5.4 Conversion of state space model to linear time varying model.....	44
5.5 Converting nonlinear state space system to linear time varying system.....	45
5.6 Solution for the linear time varying system.....	45
5.7 Matlab Simulink implementation.....	48
35Figure 5.2: Matlab Simulink implementation of the state space model.....	48
5.8 Testing devices and arrangement.....	49
5.9 Deriving state of charge from OCV.....	50
5.10 Tests & Results.....	51
5.10.1 Comparison of SOC estimated with SOC calculated from coulomb counting.....	51
5.10.2 Impact of x20 on the calculation.....	52
5.10.3 Charging case.....	53

5.10.4 Charging profile with non-charging intervals.....	54
5.10.5 Two batteries in series (Battery A & Battery C) - Discharge case.	54
Chapter 6.....	56
Prediction of end of discharge (EOD) based on voltage gradient.....	56
6.1 Battery cut-off voltage in a series of batteries.	57
6.1.1 Batteries in series discharge at 0.25C.	57
6.1.2 Batteries in series discharge at 0.5C.	58
6.1.3 Batteries in series discharge at 1 C.	59
6.2 Remaining capacity in the battery after knee point is reached.....	60
6.3 The rate of change of voltage drop to estimate the new knee voltage cut-off point.....	61
6.4 Difference of the rate of change of voltage drop to estimate the new knee voltage cut-off point.	63
Chapter 7.....	64
Conclusion.....	64



University of Moratuwa, Sri Lanka.
 Electronic Theses & Dissertations
www.lib.mrt.ac.lk

LIST OF FIGURES

Figure 1.1 : 5kW Solar installation for 25kWh daily house hold electricity consumption, with 7Kwh battery storage.[2].....	2
Figure 1.2 Hybrid off-grid inverter schematic with common DC bus.	3
Figure 1.3: Cycle life Vs Depth of Discharge – Panasonic Sealed Lead acid batteries hand book 2000[3]	4
Figure 1.4: Discharge current vs. Cut-off voltage– Panasonic Sealed Lead acid batteries hand book 2000[3]	4
Figure2.1: The relationship between discharge depth and lifetime in an Enersys Cyclon sealed lead-acid battery - (Source : Digi-Key).....	7
Figure 2.2: Constant voltage – Constant current charge characteristics Panasonic 4.5 Ah Sealed Lead-Acid battery	8
Figure 2.3 Trickle charge system model.	9
Figure2.4: Float charge system model.	10
Figure2.5: Residual capacity Vs Storage period[3].	11

Figure 2.6: Charge voltage Vs Temperature characteristic of typical lead-acid battery. [3] ...	11
Figure 2.7: Discharge characteristics [3]	12
Figure 2.8 : Relationship between residual charge to OCV- Panasonic 4.5Ah Sealed Lead-Acid Battery	13
Figure 2.9: Voltage of a 4.5Ah, SKC, sealed lead-acid battery after disconnecting from charging source.	14
Figure 2.10: Coup de Fouet phenomena during discharge of fully charged 4.5Ah SKC battery(ST640D).....	15
Figure 2.11: Coup de Fouet phenomena during discharge of 1080Ah battery bank at Kelanitissa Power Station, with 120Ah/200Ah flooded type lead-acid batteries.....	16
Figure 2.12: Extractable capacity of Exide A500 battery at different discharge rates.....	18
Figure 3.1 : Simple Thevenin's battery model [1].....	24
Figure 3.2 : Simple battery model modified to with internal resistances for charging and discharging cases.[1]	24
Figure 3.3 : Modified Thevenin's model of battery.[1].....	25
Figure 4.1: HIL Testing rig for battery monitoring and charge/discharge controlling	28
Figure 4.2: Measurement circuit diagram	29
Figure 4.3: Measurement circuit media components.....	29
Figure 4.4: PSI8080 remote controllable programmable power supply	30
Figure 4.5: EL975 remote controllable programmable electronic load	31
Figure 4.6: Simulink program.....	32
Figure 4.7: Remote communication – EL9750 and PSI8080	34
Figure 4.8: Elektroautomatic remote controllable electronic load and power supply rack.....	34
Figure 4.7: Cut off voltage for batteries against the charging current. [3].....	37
Figure 4.8: Picolog High Resolution Data Logger ADC-20 and Terminal Board.....	38
Figure 4.9: Picolog High Resolution Data Logger hardware.....	38
Figure 4.10: Flow diagram of Load profile setter sub system	40
Figure 4.11: Program flow chart- PICO measurements.....	39
Figure 4.12: Hardware arrangement of charge-discharge monitor with HIOKI 8860 device	41
Figure 5.1: Modified Thevenin's equivalent circuit model.[1]	42
Figure 5.2: Matlab Simulink implementation of the state space model.....	49
Figure 5.3: Estimation of SOC using OCV and Coulomb counting	51
Figure 5.4: Testing of the system for different initial values of X20.....	52
Figure 5.5: Estimation of VOC for charging case.....	53
Figure 5.7: Estimation of VOC for charging case with no charging intervals.....	54

Figure 5.8: Terminal voltage of two batteries discharged in series.	55
Figure 5.9: Estimated OCD of two batteries discharged in series.	55
Figure 6.1: Battery A,B & C under 0.25C discharge.	58
Figure 6.2: Battery A,B & C(Weak) under 0.5C discharge.	58
Figure 6.3: Battery A,B & C(Weak) under 1C discharge.	59
Figure 6.4: Battery discharged at different rates until respective safe cut-off levels.....	60
Figure 6.5 : Terminal voltage against rate of change of Terminal voltage at 0.25C.....	61
Figure 6.6: Terminal voltage against rate of change of Terminal voltage at 0.5C.....	62
Figure 6.7 : Terminal voltage against rate of change of Terminal voltage at 1C.....	62
Figure 6.8 : Difference of rate of change of voltage of two batteries near knee point.....	63

LIST OF TABLES

Table 1Table 2.1: Battery bank test results after 4 Hr on a 12Hr discharge test.....	16
Table 2Table 3.1: Capacity of a 20Ah battery at different discharge rates as a percentage of nominal 20 hour rate.	22
Table 3Table 4.1: Charging voltages for different batteries at different ambient temperature	36
Table 4Table 5.1: Batteries used for testing work.	49
Table 5Table 6.1: Typical End of Discharge voltages of 10Ah Lead Acid Battery	56
Table 6Table 6.2: Comparison of batteries under test.	57
Table 7Table 6.3: Percentage of unrecovered energy at different discharge rates.	60

INTRODUCTION

1.1 Background

Lead-acid batteries has being the choice for automotive applications for applications such as starting, lighting and ignition where a high power is required for a short period of time. But for energy storage applications they suffer from a shorter cycle life and typical usable power down to only 50% Depth of Discharge (DOD). With the entry of deep-cycle batteries, which can go for DOD of 75% the choice of lead-acid batteries has not being limited to automotive applications. They are also now being used for energy storage for small-scale photo-voltaic (PV) systems in the developing world, allowing electricity to be supplied when generation is not occurring. But the batteries often account for a as much as 20% of the capital cost of such small scale renewable energy system and also have the shortest lifetime when compared to other components. With this high costs of storage for solar energy, the developing trend has being to supply electricity to the grid during day time and absorb electricity from grid supply the night time, during which the electricity is produced by running expensive thermal power plants. Hence the addition of domestic solar has not contributed effectively to ease the burden on grid in Sri Lanka. Coupling the house hold solar energy system with a battery storage can support to store solar energy during peak solar production hours to supply and share the loads during the peak-energy hours. Figure 1.1 illustrate production and consumption curves of typical solar installation coupled with a battery storage system.

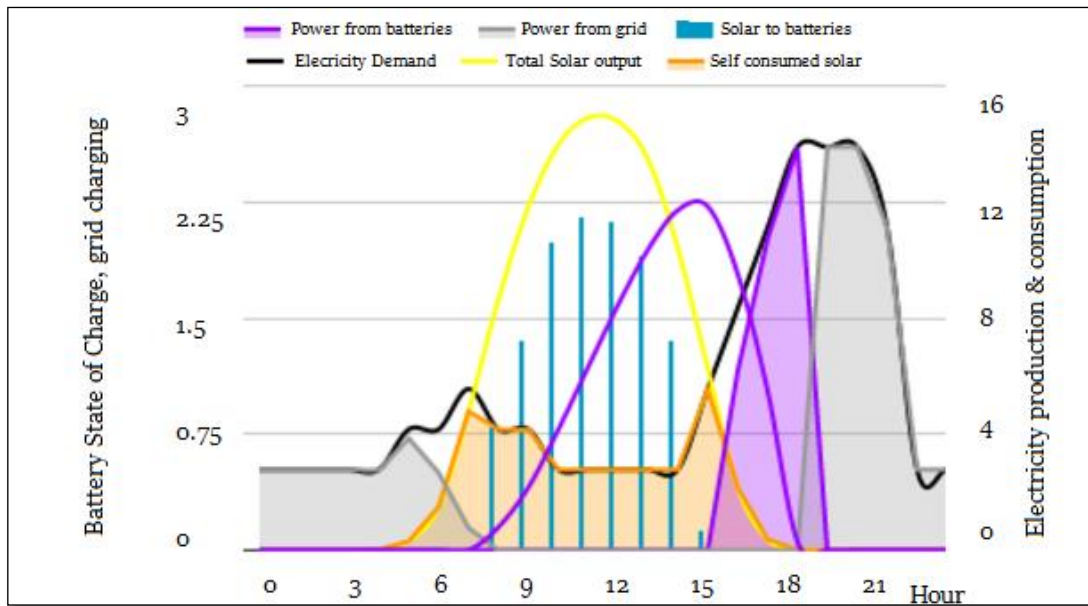


Figure 1.1 : 5kW Solar installation for 25kWh daily house hold electricity consumption, with 7Kwh battery storage.[2].

For a domestic solar installation of 1kw which may typically estimate to produce 120 kwh per month, it would be typical to install 3 no of 120Ah 12V lead acid batteries to store the produced energy safely and to supply during night times. In small solar installations of this range it would be possible to use automotive type batteries which are not very expensive compare to the cost of solar installation in that range. But dealing with lead acid batteries need to be coupled with a comprehensive battery state monitoring system to avoid undesirable cascade failures. The major disadvantage in using more than one lead-acid battery arranged in either series or parallel configuration in an installation with frequent charge-discharge cycles would be that a small weakness in one of the battery can lead to a rapid failure of the whole bank.

1.2 Identification of the Problem & Motivation

Sri Lanka is a developing nation with a large growing demand for electrical power. Majority of the energy demand(60%) is met by thermal power sources such as coal, while another 35% is met by conventional hydro power. Generation of electricity with expensive thermal power sources have put lot of pressure on the economy with limited no of upcoming large scale hydro power projects. In this context domestic

solar power installation has become a trend with the introduction of tariff schemes by the utility supplier to facilitate and encourage the same. Though this eases out the burden on grid to some extent it doesn't really contribute when the peak energy requirement occurs during the night. In this context the development of small scale renewable energy with storage is more desirable.

In simple systems, the management of the battery sub-system is often crude, with the battery charged directly via a solar panel through a simple reverse-blocking diode and supplying an inverter incorporating a simple under-voltage cut-out in an attempt to avoid over-discharge. This leads to frequent over-charging (and over-discharging if the voltage cut-out is set incorrectly) of batteries and early failure, necessitating costly refurbishment or replacement. Also this can cause depletion of batteries to the point that some cells are driven into reverse polarity.

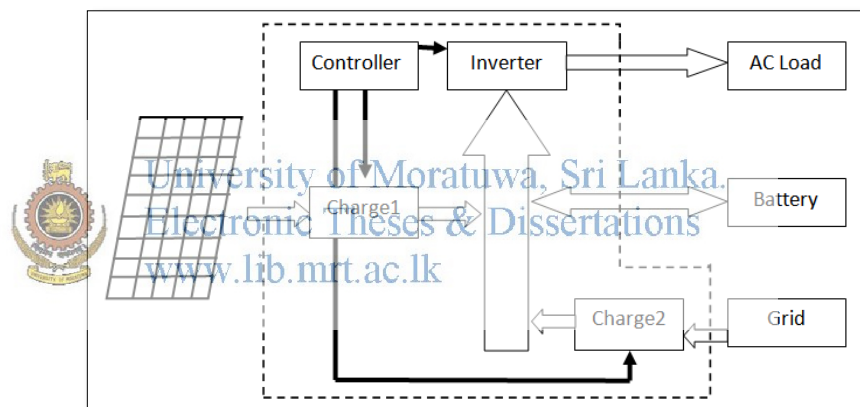


Figure 1.2 Hybrid off-grid inverter schematic with common DC bus.

Cycle life of a lead-acid battery largely depends on the depth of discharge during its discharge cycle, as depicted in figure 1.3. As per the figure if a battery is discharged to the depth of 100%, after 200 cycles its effective capacity is lost by 40% (Remaining capacity 60%). On the other hand if a batter is discharged to a depth of only 30%, it will take 1200 cycles to lose its effective capacity by 40%. Hence it is very important that the correct discharge level is maintained to save battery life cycle.

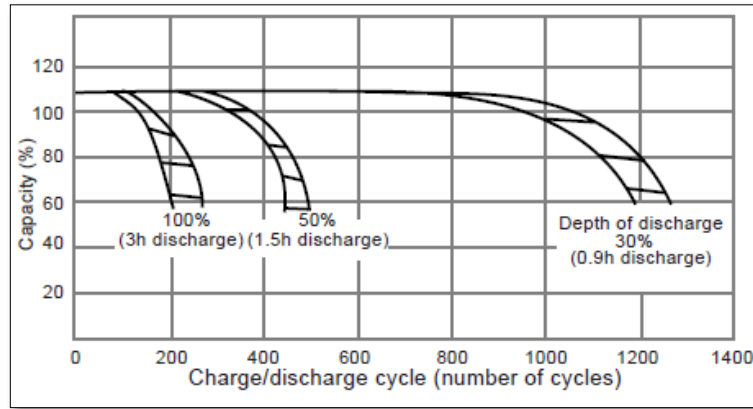


Figure 1.3: Cycle life Vs Depth of Discharge – Panasonic Sealed Lead acid batteries
hand book 2000[3]

Lead-acid battery, under volt cut off point varies depending on the rate of discharge as shown in figure 1.4. In most of the battery discharge control systems a flat discharge-cut off point is used irrespective of the rate of discharge. Discharge cut-off voltage for a 12V lead-acid battery for the discharge rate of 1C is 9.7V, whereas for a discharge rate 0.1C the cut-off voltage is 10.6V. This method can easily make a slightly weak battery in the battery pack to over discharge when discharged with a lower discharge rate, if a wrong under volt cut off point is used.

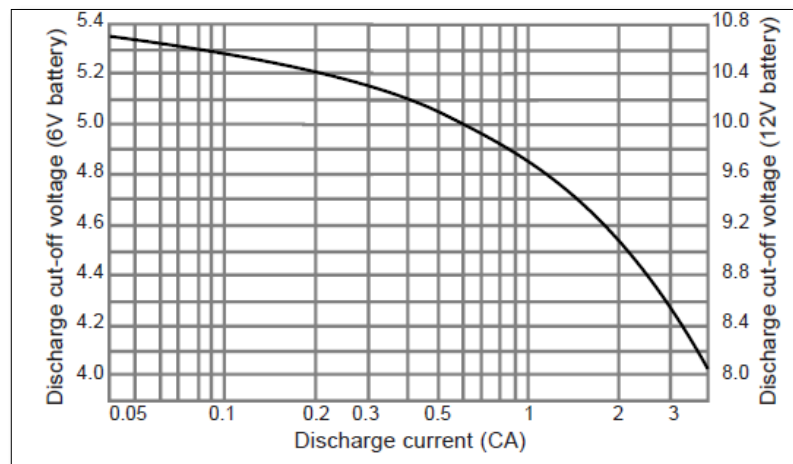


Figure 1.4: Discharge current vs. Cut-off voltage– Panasonic Sealed Lead acid
batteries hand book 2000[3]

1.3 Objective of the Study

Lead-acid batteries is one of the solution for small scale domestic solar installations with hybrid inverter controller systems. Except for deep cycle batteries, other inexpensive batteries are usually discharged to the depth of 40%-50% to save the cycle life. Cycle life of lead-acid batteries have pose a major challenge for the users, with the risk of cascade failures, incurring costly replacements. Knowledge of SOC of battery in real time can reduce this risk by large fraction. There are different methods and techniques developed for determination of state of charge of lead-acid batteries which vary from basic methods such as coulomb counting to highly sophisticated methods such as impedance tracking. The objective of the thesis is to study a suitable method which is applicable for the above particular application of series installation of lead acid batteries to estimate the state of charge and predict safe discharge cut off point.

1.4 Methodology

This thesis thoroughly investigate the applicability of control theory based approach based on modified Thevenin's model for batteries, proposed by John Chiasson in paper "Estimating the State of Charge of a Battery"[1], where it considers only terminal voltage and current of the battery for estimating state of charge. A Matlab Simulink model was constructed and a hardware in the loop(HIL) test setup was developed in Simulink interfacing external hardware devices and sensors for real time testing of battery charging/discharging. Offline test setup was also developed for long run tests, using HIOKI high precision memory recording device. Tests were carried out for different setups of batteries under difference conditions.

LEAD ACID BATTERY CHARACTERISTICS.

2.1 Aging of battery.

Aging is the depletion of a battery usable capacity can drop due to natural reasons during usage as well as unhealthy ways of operating batteries. Anodic corrosion and sulfation are very common factors that cause aging which are also inter-dependent. The rates of the different aging processes strongly depend on the type of use (or misuse) of the battery. Over-charge will lead to accelerated corrosion and also to accelerated loss of water whereas over-discharge during cycling results in accelerated positive active mass degradation.

2.2 Battery depth of discharge Vs cycle life.

Depth of discharge of battery is one of the crucial determinant in deciding its cycle life. Cycle life expressed here is the no of charge discharge cycles before its actual effective capacity falls below 80% of its initial rated capacity. At a given temperature and discharge rate, the amount of active chemicals transformed with each charge-discharge cycle will be proportional to the depth of discharge. The relation between the cycle life and the depth of discharge appears to be logarithmic as shown in the graph below. Lead acid batteries are typically specified a recommended maximum depth of discharge for their nominal cycle lifetime (e.g. 1,000 cycles at a DOD of 50%).

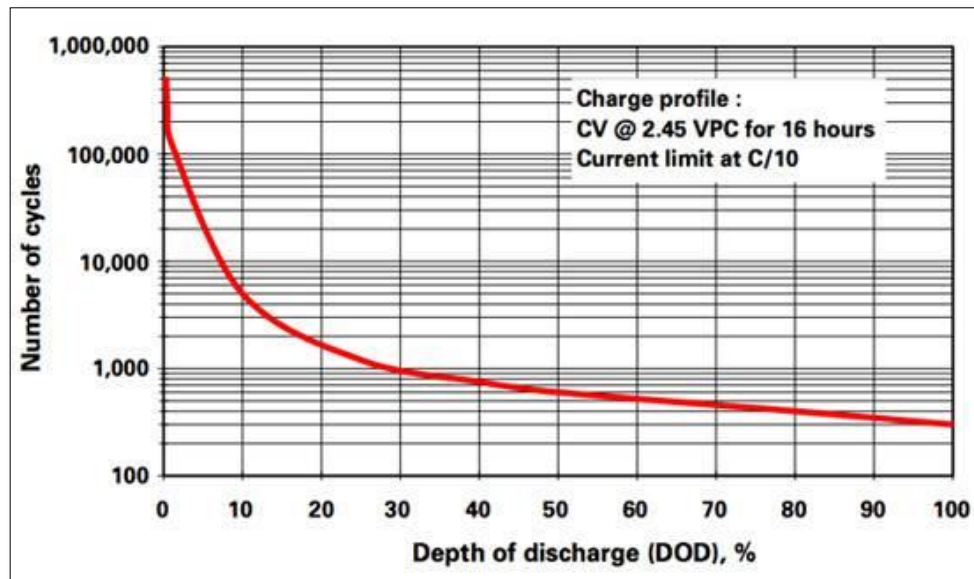


Figure 2.1: The relationship between discharge depth and lifetime in an Energys Cyclon sealed lead-acid battery - (Source : Digi-Key)

2.3 Battery charging.

Charging methods of a battery depend on battery applications and applications area roughly classified into main power (cycle use) applications and backup power (standby use) applications.

2.4 Main power (Cycle use)

Cycle use is to use battery by repeated charging and discharging. In main power applications also batteries are charged in two methods as to constant voltage charging and constant voltage - constant current charging method.

2.4.1 Constant voltage charging method

This method is to charge the battery by applying a constant voltage between the terminals. Typical specified voltage for charging a battery is applying a voltage of 2.45V per cell (unit battery). This way the current is not controlled and it will allow the current to take the natural profile control by its self impedance. Charging is considered complete when the charging current continues to be stable for 3 hours. Valve regulated lead acid batteries can be easily over charged without the regulation

and control of voltage. When a battery is overcharged water in the electrolyte is decomposed by the electrolysis and generates more oxygen than what can be absorbed by the negative electrode. This makes the electrolyte lost as oxygen and hydrogen from the battery system. As the quantity of the electrolyte is reduced chemical reactions of charge and discharge become inefficient and hence the battery performance is severely deteriorated. Therefore it is important that the exact voltage specified is maintained and also the charging time is controlled.

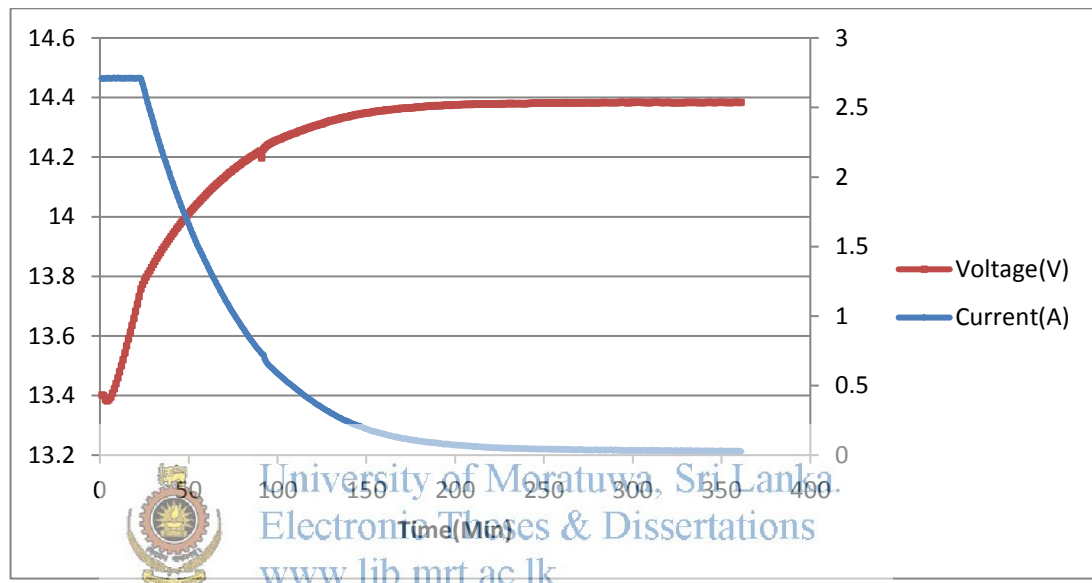


Figure 2.2: Constant voltage – Constant current charge characteristics Panasonic 4.5 Ah Sealed Lead-Acid battery

2.4.2 Constant voltage – constant current charging method

This method charges the battery by controlling the current and also controlling voltage at 2.45V/Cell. There will be two distinguishable stages during the whole process of charging until the whole battery is charged. During first stage the charging current will be a constant while the terminal voltage is building up till the specified voltage (Control voltage) 2.45V/cell is reached. In the second stage, after the terminal voltage reaches the specified voltage, the charging current will gradually go down until it reaches a stable low current like 30mA. Normally the same voltage is maintained for another 3 hours to pump in the final charge to the battery(Topping charge). So the initial stage of the charging will be a constant current region where

the terminal voltage gradually builds up which will be followed by a stage where the voltage will be consistent while the charging current gradually decreases.

2.5 Standby / Back up use charging

Stand by use is to maintain a battery system at all times so that it can supply power to the load in case main supply mean fails. Mainly in this method the battery is disconnected from the load and kept charged with a small current only for compensating self discharge while main power is alive. In case of power failure the battery is connected to deliver the load. In normal charging state (trickle charge state), 2.3V/cell is typically maintained as the charging voltage to supply the self discharge. But if a rapid recharge is required either one of the methods as in cycle use can be used to charge the battery at a higher current level.

2.5.1 Trickle charge system.

In this charge system, the battery is disconnected from the load and kept charged with a small current as shown in figure 2.3. This voltage is selected sufficient for compensating the self discharge when not in use. The battery is automatically connected to the load when the main power fail. This system is applied mainly as a spare power source for emergency equipment. In this use, if rapid recovery of the battery after discharge is required, it is necessary to consider the recovery charge with a comparatively large current followed by trickle charge, or alternative measures.

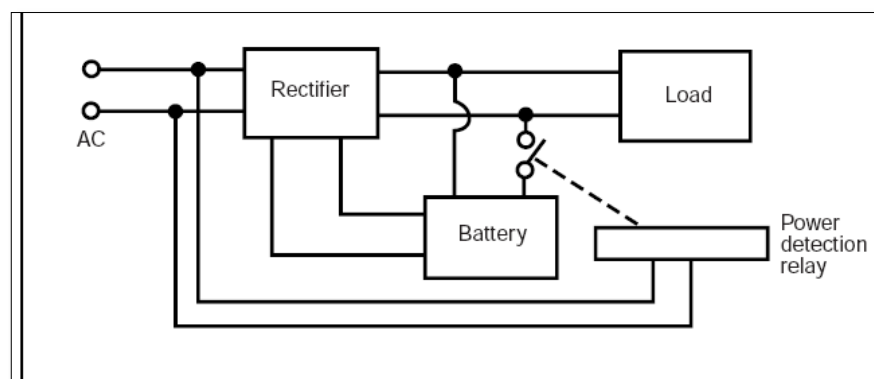


Figure 2.3 Trickle charge system model.

2.5.2 Float charge system.

Float charge system is a one where the battery and the load are connected in parallel to the rectifier which should supply a constant current. Even in float charge systems a voltage of 2.3V/cell is maintained and this voltage needs to be very precisely controlled since the charging voltage is always present. A slight error in the charging voltage can cause the life of the battery to reduce drastically. In the illustrated model in figure 2.4, output current of the rectifier is expressed as the addition of I_c and I_L , where I_c is charge current and I_L is load current. In the float system, capacity of the constant-voltage power source should be more than sufficient against the load. Usually, the rectifier capacity is set as the sum of the normal load current plus the current needed in order to charge the battery

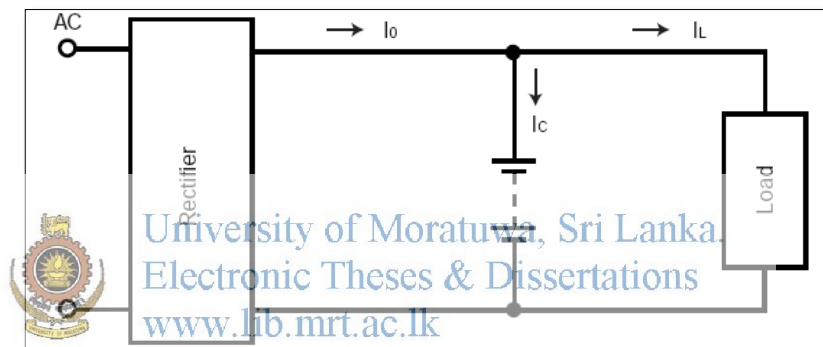


Figure2.4: Float charge system model.

2.6 Self discharge and refresh charge.

During storage, batteries gradually lose their capacity due to self discharge, therefore the capacity after storage is lower than the initial capacity. This effect is enhanced by the ambient temperature where the self discharge rate doubles for each 10 degree Celsius rise of temperature. For the recovery of capacity it is usually recommended to repeat charge/discharge several times.

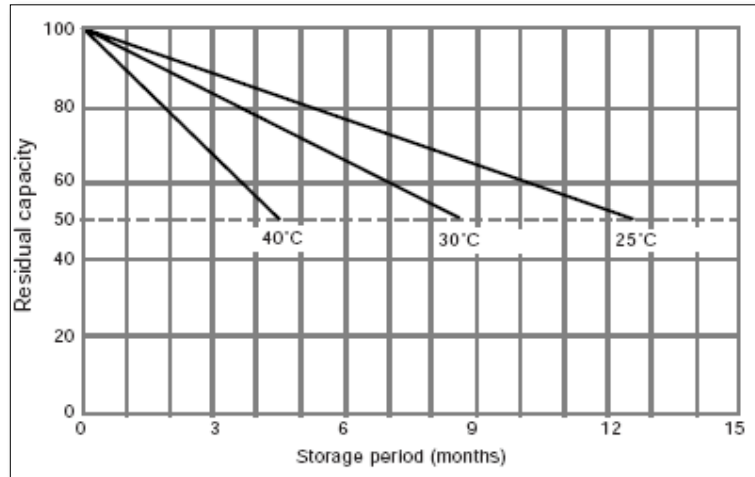


Figure 2.5: Residual capacity Vs Storage period[3].

2.7 Charging voltage and the ambient temperature.

The charging voltages of a battery vary depending on the ambient temperature it is exposed to. The battery manufacturers usually provide with a graph as shown in figure 2.6 to indicate different voltages for charging in different applications and in different ambient temperatures.

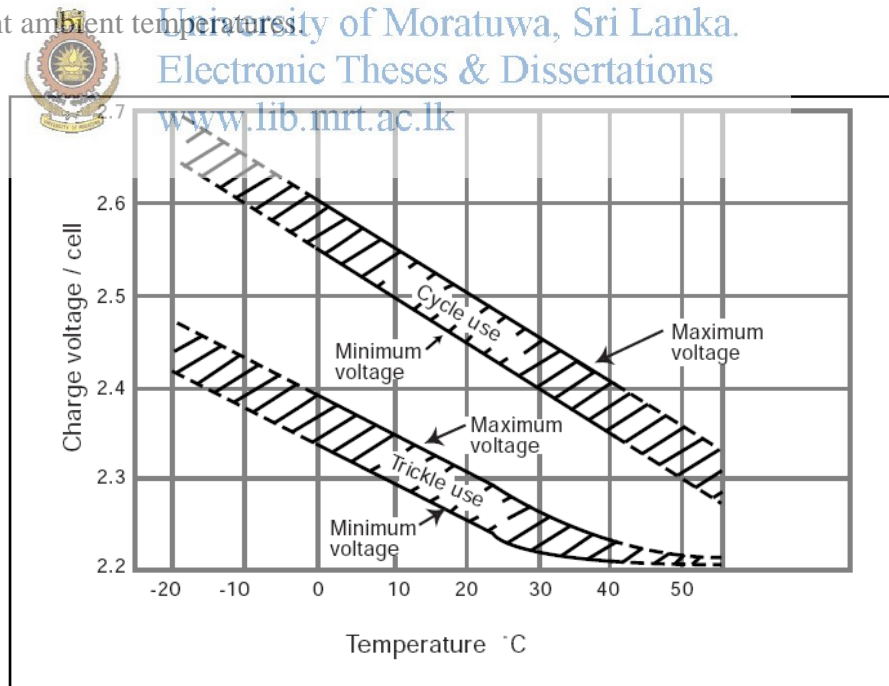


Figure 2.6: Charge voltage Vs Temperature characteristic of typical lead-acid battery. [3]

2.8 Discharging of a lead acid battery.

Discharging of a battery at a constant current follows distinguishable two stages. During the first stage the battery delivers a constant current while also maintaining the terminal voltage. During the second stage the battery is not capable of maintaining the terminal voltage but delivers the current. During this stage a faster drop in the voltage can be observed and this needs to be limited before it goes below the cut off voltage that the manufacturer has recommended.

Recommended cut-off voltages for 12V, 4.5Ah sealed lead acid battery consistent with discharge rates are given in the figure 2.7. With smaller discharge currents, the active materials in the battery work effectively, therefore discharge cut-off voltages are set to the higher side for controlling over discharge. For larger discharge currents, on the contrary, cut-off voltages are set to the lower side. A slight over discharge of a battery can sacrifice a significant portion of its useful life time.

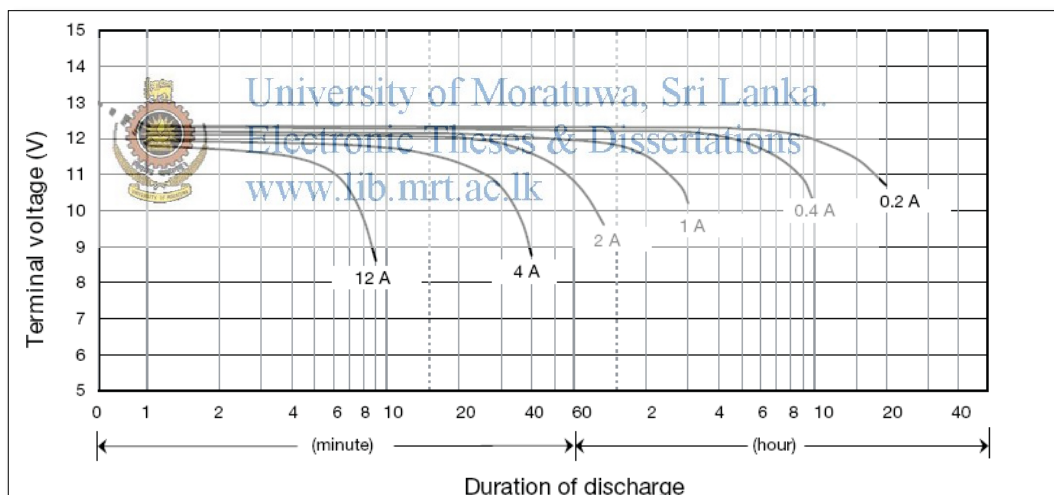


Figure 2.7: Discharge characteristics [3]

2.9 Open circuit voltage of a battery.

Open circuit voltage (OCV) of a lead acid battery shows a linear relationship to its residual capacity. Figure 2.8 shows the relationship of residual charge to OCV for a Panasonic, 4.5 Ah, 12V sealed lead acid battery, extracted from a manufacturer's datasheet. Voltage at residual capacity of 100% can also be experimentally find out by letting a fully charged battery to settle down and measuring the OCV. And OCV

at residual capacity of 0% can also be found experimentally by measuring the OCV after completely draining a battery.

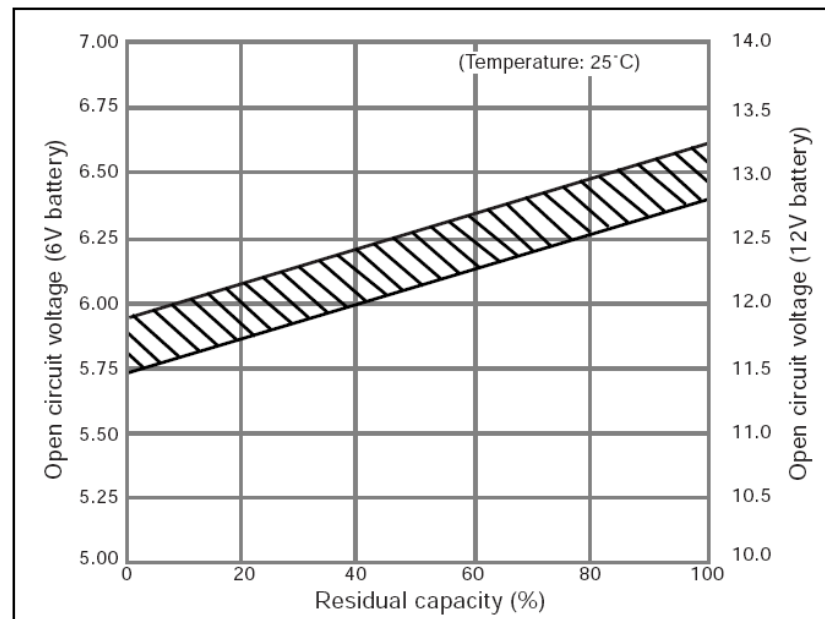


Figure 2.8 : Relationship between residual charge to OCV- Panasonic 4.5Ah Sealed



University of Moratuwa, Sri Lanka.
Electronic Theses & Dissertations
www.lib.mru.ac.lk

Although open circuit voltage of a battery is an accurate method of estimating the state of charge of a battery, its difficult to utilize this in a real time application since it is difficult to measure the OCV by disconnecting the circuit and also even if the circuit is disconnected the it takes considerable amount of time to stabilizes to a constant voltage. This effect is elaborated in the Figure 9 which shows the voltage of a battery before and after disconnecting from a load.

2.10 Open circuit voltage of a battery against stabilization time.

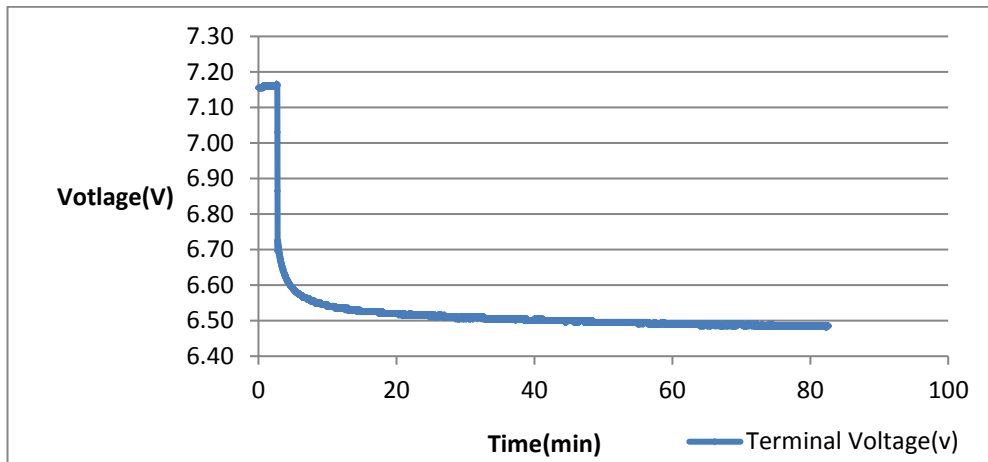
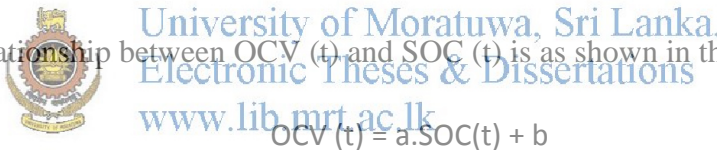


Figure 2.9: Voltage of a 4.5Ah, SKC, sealed lead-acid battery after disconnecting from charging source.

2.11 Relationship between open circuit voltage (OCV) and state of charge(SOC).

If the relationship between OCV (t) and SOC (t) is as shown in the equation (2.1) [1],


$$OCV(t) = a \cdot SOC(t) + b \quad (2.1)$$

Where 'a' is the open circuit voltage at 100% SOC and 'b' is the open circuit voltage at '0%' SOC. These two known points which can either be experimentally found or can get from manufacturers test results will give a good estimate of the battery state of charge at given instant.

2.12 Coup de fouet region.

Coup de fouet is an phenomena associated with voltage drop in the early minutes of lead-acid battery discharge. At the start of discharge the voltage drops to a minimum, or trough. This occurs in a relatively short time, in the order of a few seconds to a few minutes, depending on the discharge conditions (primarily discharge rate). The voltage then recovers in an exponential fashion, to level off or plateau, after a further few minutes. Then it takes the usual downward profile if the load it supply is persistent.

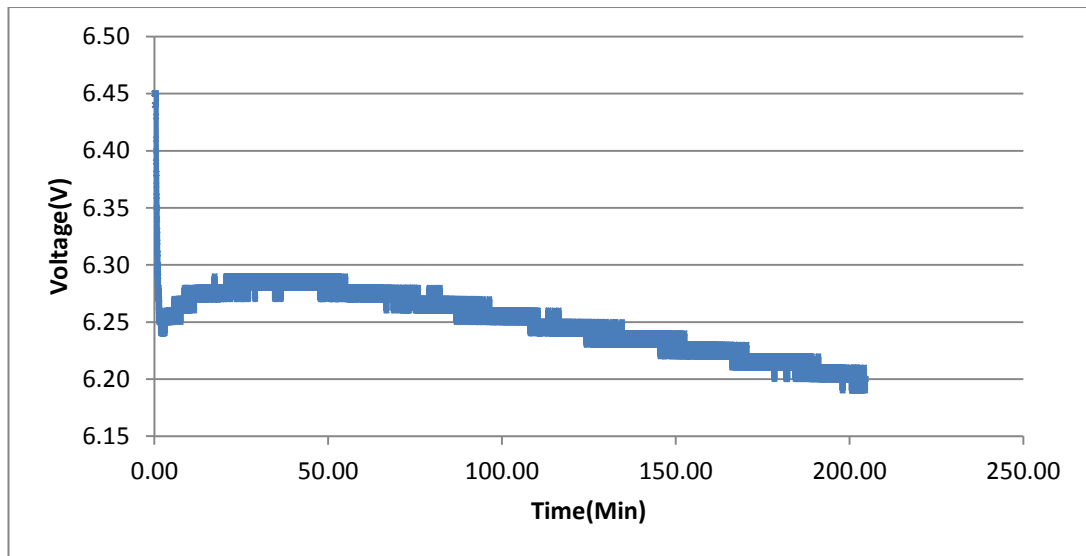


Figure 2.10:Coup de Fouet phenomena during discharge of fully charged 4.5Ah SKC battery(ST640D).

In some applications where a high power is required during the initial stage of the loading the trough voltage of the coup de fouet can be lower than the required end voltage when the batteries are in series. To avoid this some schemes are devised with the intention of eliminating the need for extra cells within the battery to compensate for the voltage drop during the trough region. Coup de Fouet phenomena is subjected to recent research work to analyzing its effectiveness in estimating the health of a battery. This relationship it yet to directly reveal the health of a battery as Coup de Fouet voltage dip depends on several other factors also, such as rate at which the discharge is done. But several batteries in the same bank with same age under same stress shows close correlation between its health and Coup de Fouet voltage as illustrated in figure 2.11.

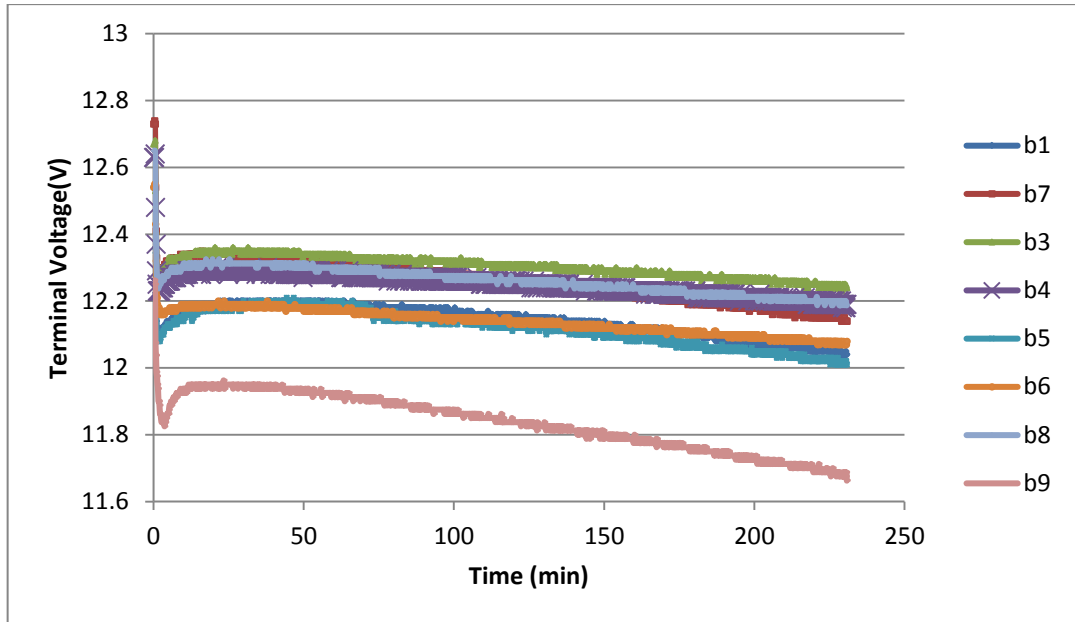


Figure 2.11: Coup de Fouet phenomena during discharge of 1080Ah battery bank at Kelanitissa Power Station, with 120Ah/200Ah flooded type lead-acid batteries.

Battery no b9 showed a deep Coup de Fouet voltage as well as significant deviation during 12Hr load test. This particular battery reached to its final voltage of 11.82V after around 4 hours, where the initial OCV before test was measured as 12.8V.



University of Moratuwa, Sri Lanka.
Electronic Theses & Dissertations
www.lib.mrt.ac.lk

No	Terminal Voltage at Float charge before test.	Terminal Voltage at Open Circuit before test.	Terminal Voltage at Open Circuit after test
b1	13.3	12.9	12.06
b3	13.3	13.0	12.30
b4	13.2	13.0	12.25
b5	13.2	12.9	12.06
b6	12.7	12.6	12.24
b7	13.6	13.1	12.13
b8	13.4	13.0	12.27
b9	12.9	12.8	11.82

Table 2.1: Battery bank test results after 4 Hr on a 12Hr discharge test.

2.13 Overcharging

As a result of too high a charge voltage excessive current will flow into the battery, after reaching full charge, causing decomposition of water in the electrolyte and premature aging. At high rates of overcharge a battery will progressively heat up. As it gets hotter, it will accept more current, heating up even further. This is called thermal runaway and it can destroy a battery in as little as a few hours.

2.14 Undercharging

If too low a charge voltage is applied, the current flow will essentially stop before the battery is fully charged. This allows some of the lead sulfate to remain on the electrodes, which will eventually reduce capacity. Batteries which are stored in a discharged state, or left on the shelf for too long, may initially appear to be “open circuited” or will accept far less current than normal. This is caused by a phenomenon called “sulfation” . When this occurs, leave the charger connected to the battery. Usually, the battery will start to accept increasing amounts of current until a normal current level is reached. If there is no response, even to charge voltages above recommended levels, the battery may have been in a discharged state for too long to recover.

2.15 Discharge rate Vs Extractable energy

Charge and discharge rates of a battery are usually expressed in C-rates. The capacity of a battery is commonly rated at 1C, meaning that a fully charged battery rated at 1Ah, discharged at 1C should be able to supply a steady current of 1A for one hour. The same battery discharging at 0.5C should provide 500mA for two hours, and at 2C it delivers 2A for 30 minutes. Losses at fast discharges reduce the discharge time and these losses also affect charge times. Manufacturers of batteries specify extractable capacity at different discharge rates.

To obtain a reasonably good capacity reading, manufacturers commonly rate lead acid batteries at a very low 0.05C, or a 20-hour discharge. Even at this slow discharge rate, lead acid seldom attains a 100 percent capacity as the batteries are overrated as illustrated in figure 2.12.

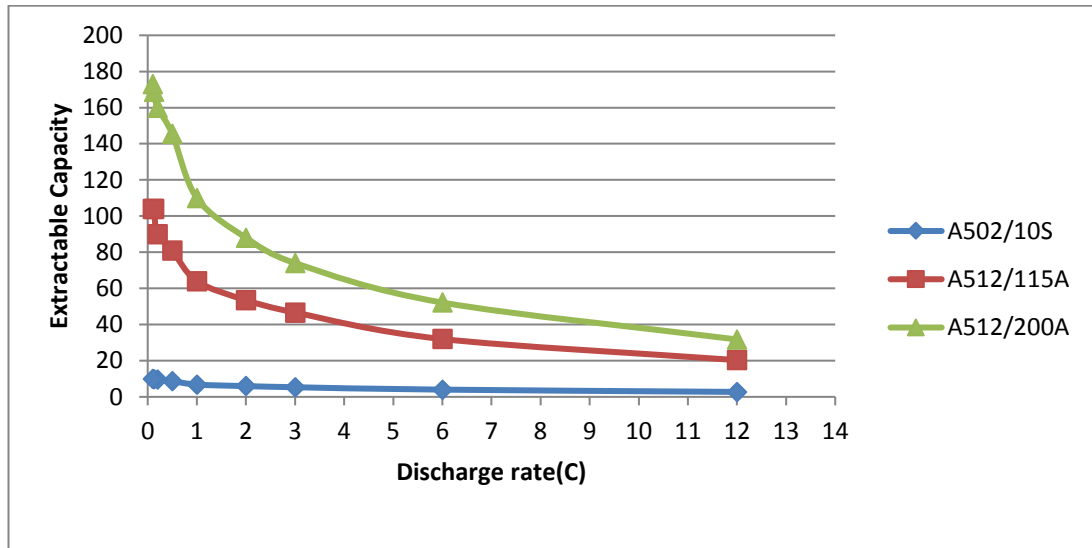


Figure 2.12: Extractable capacity of Exide A500 battery at different discharge rates.



BATTERY STATE OF CHARGE ESTIMATION TECHNIQUES.

A lot of research efforts have gone into determining of precise state of health parameters of VRLA batteries. Battery performance indicators such as residual capacity and reserve charge cannot be measured directly, though many methods have being evolved and devised. Still only way to determine exact residual capacity of a battery is to perform full discharge-charge tests as per battery manufacturers discharge tables and guide lines. But such capacity tests need to disconnect the array or battery bank from the loads which is a not very practical approach. However there are different methods which have being developed to do this while the batteries are still online. All of these methods have their own advantages and disadvantages. Also the applicability of methods depend on the applications too. This chapter will discuss such methods that are developed to measure state of batteries and applicability of the techniques for a VRLA batteries in a series array in the lines of applicability for small scale installations for storage of energy generated from domestic solar power.

3.1 Open circuit discharge test.



University of Moratuwa, Sri Lanka.
Electronic Theses & Dissertations
www.lib.mrt.ac.lk

Complete discharge test is recognized as the most reliable method to determine the existing effective capacity of a battery pack. It is recommended to carry out the test at Intervals which are not greater than 25% of the expected service life or two years, whichever is less. Batteries in string are taken off discharged through a large load to an end voltage. Then the discharge time is compared to manufactures specification at initial point. It is a norm that a discharge time in excess of 80% of initial discharge time prove the satisfactory performance of a battery pack. This process will take longer outage of battery pack, expensive bulk load discharge equipment and labor also. In addition to that individual cell performance will not be revealed by this test. On the other hand a weaker cell can be fully stressed to its failure point on a deep discharge test like this.

Due to above disadvantages a modified method of discharge test have being developed[12]. This method required only to carry out a partial discharge test of duty cycle multiplied by the aging margin used in sizing the battery specified by the battery manufacturer.

$$\% \text{ Capacity at } 25^{\circ}\text{C} = [t_A / (t_s \times K_T)] \times 100 \quad (3.1)$$

where ,

t_A = actual time of test to specified terminal voltage

t_s = rated time to specified terminal voltage,

K_T = correction factor for the electrolyte temperature prior to the start of the test.

Though this method reduces the other difficulties and disadvantages discussed in full discharge test this also reduces the accuracy of the test by around 20% [9]. The equation (3.1)[12] is used to determine the battery capacity for an acceptance test or a modified performance test that runs 1 hour or longer for the time adjusted method. For both discharge tests a temperature correction has to be done to the capacity calculation after completion of the test using recommended time correction factor K_T as per Table 1 of IEEE Std 450-2002.

3.2 Coulomb counting method.

Coulomb counting technique[16] estimates the reserve capacity by accumulating the charge and discharge currents. The initial remaining capacity will be the end remaining capacity of previous test. A factor α is introduced here to compensate for charging efficiency based on battery temperature and charge status. Identifying the charge status is important as the charge efficiency is very high early on in the charge phase but reduces gradually at the float charge phase. Also when the battery is being discharged α represents a compensating factor that adjusts the reserve charge in accordance with the particular discharge current and battery temperature. Discharging at a higher rate can retrieve lesser current compared to discharging at a lower rate as shown in the table 3.1.

$$\text{SOC} = \frac{\sum_{t_0}^t I_b(\tau) d\tau}{Q_{Q_0}} \times 100 \quad (3.2)$$

Coulomb counting methods require to always remember the previous state of charge(SOC) and measure of reserve charge. This is normally found by performing a full discharge test at one point before the actual tests begin. The efficiency factor α is also found experimentally, and require many iterations to determine its values, for the different range of operating conditions and applications. Hence this method is practically difficult to implement in a application where the conditions differ continuously. Also with the aging of batteries factor α need to be updates to avoid giving wrong estimates of reserve capacities.

Biggest disadvantage of this charge accumulation method is that it require to remember the previous states of charge discharge and unable to estimate the states in a single standalone measurements. Any errors produced in each iteration can accumulate and produce wrong results too if done without frequent full discharge tests to correct the reserve capacities. Hence this method has proved to be not reliable for estimating the state of charge (SOC) accurately.

3.3 Peukerts equation based method.

These methods devise models and verify them using experimental and observation data. Peukerts behavioral model is one of most widely used such method, which relates battery capacity to rate at which the battery is discharged [4][5]. Typically any battery manufacturer will state different rates at which their batteries can be discharged and how much power can be extracted at these different levels. The most common discharge rate for any battery is 20 hour rate and other capacities are shown as percentage of 20 hour rate. Also together with this, the cutoff voltage is also specified in per cell basis as shown in the table 3.1 for Exide-German batteries.

Discharge time t_n	10 min	30 min	1 h	3 h	5 h	10 h	20 h
Capacity C_n [Ah]	$C_{1/8}$	$C_{1/2}$	C_1	C_3	C_5	C_{10}	C_{20}
Capacity in % of the nominal capacity C_{20}	40 %	50 %	55 %	80 %	83 %	86 %	100 %
U_f in Volt per cell	1.60	1.70	1.74	1.78	1.79	1.80	1.75

Example:

$$C_3 (S 512/25) = 80 \% * 25 \text{ Ah} = 20 \text{ Ah}$$

Table 3.1: Capacity of a 20Ah battery at different discharge rates as a percentage of nominal 20 hour rate. [6]

As the table depict a 100Ah battery at 20 hour discharge rate would give 5A for 20 hours as this allows for complete 100% discharge. But discharge at 10 hour rate would not be able to give a give a current of 10A as at this rate extractable capacity is only 86%. The Peukerts equation constructs a formula to relate this relationship given that the Peukerts exponent is available from manufacturers data or experimental results.

Peukerts equation is expressed as $C = \frac{C_{20}}{I^n T^n}$ (3.3)

where,

I = the discharge current in amps

T = the time in hours

C = the capacity of the battery in amp hours

n = Peukert's exponent for that particular battery type

There are currently several techniques devised for predicting the reserve charge of a lead-acid battery discharged with a variable current based on different variants of Peukert's equation. Most of these methods relates the available capacity to a constant discharge current and dynamically update and predict the reserve charge. It was noted that the Peukert's equation was applied in many research papers and applications in the wrong way considering the 20 hour rate(0.05C) as the base rate, where as original Peukert's exponent is given for 1 hour rate(1C). Thus some research papers conclude that Peukert's equation cannot be used to predict the state of

charge of a battery accurately unless it is discharged at a constant current and constant temperature. [7]. However in respect of the scope of this thesis, method of prediction based on Peukert's equation still require to keep track on state of charge from the last charge or discharge state of battery. Which again is be subjected to same errors such as in coulomb counting methods. Wrong starting state of charge can predict a wrong state of charge of a battery.

3.4 Observation and behavioral methods.

Observation behavior type method is to relate the discharge voltage gradient to reserve time t_r , as described in equation (3.41) [8]. $V(t_1)$ and $V(t_2)$ are discharge voltages at discharge times t_1 and t_2 respectively. The scaling factor n depends on the different end voltages V_E .

$$t_r = \frac{V(t_1) - V_E}{\left\{ \frac{n(V(t_1) - V(t_2))}{t_1 - t_2} \right\}} \quad (3.4)$$

This method is simple and relatively accurate, but its performance depends on the appropriate determination of the scaling factor n . Also the main disadvantage in this context of thesis is that this method can predict the reserve capacity only for a stable discharge current and its not applicable for estimating under varying current.

3.5 Battery electrical models.

The mostly used simple battery model consist of an ideal battery with an open circuit voltage of V_o , a series resistance R_i and terminal voltage of V_b . R_i represents the overall internal resistance of the battery. With this simplest model R_i can be deduced by measuring the open circuit voltage before a start of a test and measuring V_b during a test in the close circuit. But it has its own drawback that the R_i varies with the charge –discharge current conditions and also open circuit voltage cannot be dynamically measured during the test to update this R_i value.

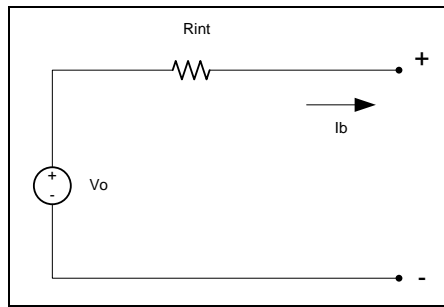


Figure 3.1 : Simple Thevenin's battery model [1]

To cater for this drawback above model is slightly modified and used in some simple applications where only a rough estimate of R_i required and there by determine the state of charge. The difference from the previous model being an introduction of two different resistances for charge and discharge scenarios.

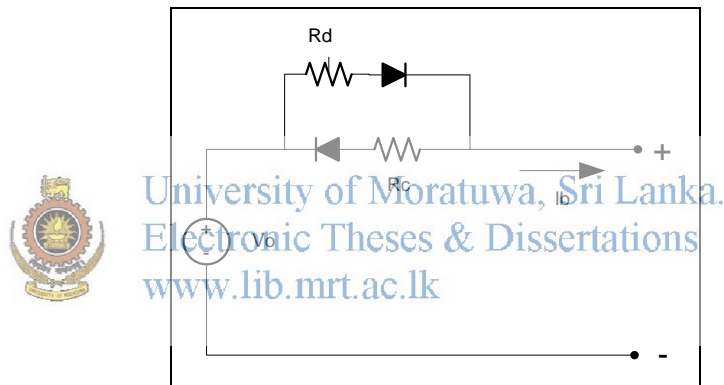


Figure 3.2 : Simple battery model modified to with internal resistances for charging and discharging cases.[1]

Yet this model has the drawback stated in previous model and does not represent the diffusion of electrolytic through the battery and its result effect of flowing of current internally. A parallel capacitor is introduced in the modified model to model this behavior as shown in the figure 3.3 bellow. Also a resistance R_b models the internal resistance which R_d and R_c model the discharging and charging losses. Applicability of this model is analyzed with experiments in this thesis as this model represents a dynamic behavior of a battery which can be modeled for any state of a battery during charge or discharge scenarios.

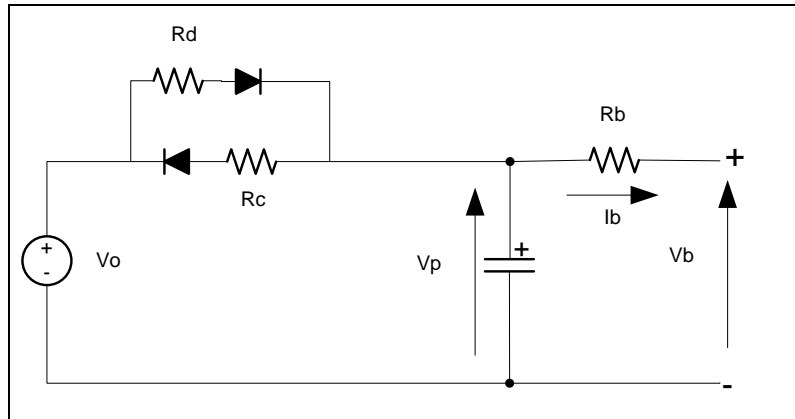


Figure 3.3 : Modified Thevenin's model of battery.[1]

- Resistance R_c , for accounting for electrical and non-electrical losses during charging.
- Resistance R_d , for accounting for electrical and non-electrical losses during dis-charging.
- Resistance R_b , for accounting for internal resistance.
- Capacitor C , for accounting for transient current conditions.



BATTERY TEST SETUP

This chapter describes the two test setups used for testing of batteries throughout this thesis. The first method was developed for testing batteries in a fully automated way and produce estimations dynamically by carrying out dynamic calculations during charge and discharge processes. The second test setup is developed for tests where dynamic calculations are not required and further analysis of data was done after the charge –discharge tests.

4.1 Development of hardware in the loop (HIL) simulation test setup.

In the first test setup it was intended to interface external hardware such as batteries, loads and power sources to Matlab environment to enable dynamic calculations and also to automate the test processes. To develop this test setup sophisticated programmable power supplies and electronic loads which can accept different load or source profiles were used. Also a data acquisition device with 20 bit resolution and USB based communication interface was used. It was intended to automate the charge/discharge process by giving a pre-defined charge/discharge profile of any shape via Matlab. The measured parameters were acquired in real-time via data acquisition unit to feed to the estimation algorithms or calculations. The Matlab Simulink environment was intended to set charge/discharge profiles via serial communication link to these sophisticate devices. Hence a Matlab simulink based hardware in the loop test setup was developed as shown in figure 4.1.

Voltage , current and temperature are the important factors in determining the state of a battery in a given scenario. But the impact of temperature was considered in this as the typical temperature throughout the year is within a range of 5 degrees Celsius.

The developed system continuously monitors the voltage and current at a given resolution with any current profile for charging or discharging of the battery that the user feeds in to the system. Charging and discharging of the batteries were done by a remote controlled, programmable power supply (PSI8080) and electronic load (EL9750). Data acquisition is done via a programmable and remote accessible high resolution 20bit data logger (PICOLOG ADC20).

The Matlab Simulink environment was selected for the development work so that, an algorithm developed in simulink can be connected to the developed system to test their validity and for further analysis. The model runs in real-time, having synchronized the simulation clock to the PC clock in which the program is running. This way it is expected to achieve correct time synchronization that is expected in a usual hardware in the loop (HIL) testing set up. The synchronization is achieved by a special block developed to look into the pc clock and adjust the time accordingly in the simulation clock. figure 4.1 illustrates the testing setup and the devices involved in the system and how each is linked.



University of Moratuwa, Sri Lanka.
Electronic Theses & Dissertations
www.lib.mrt.ac.lk

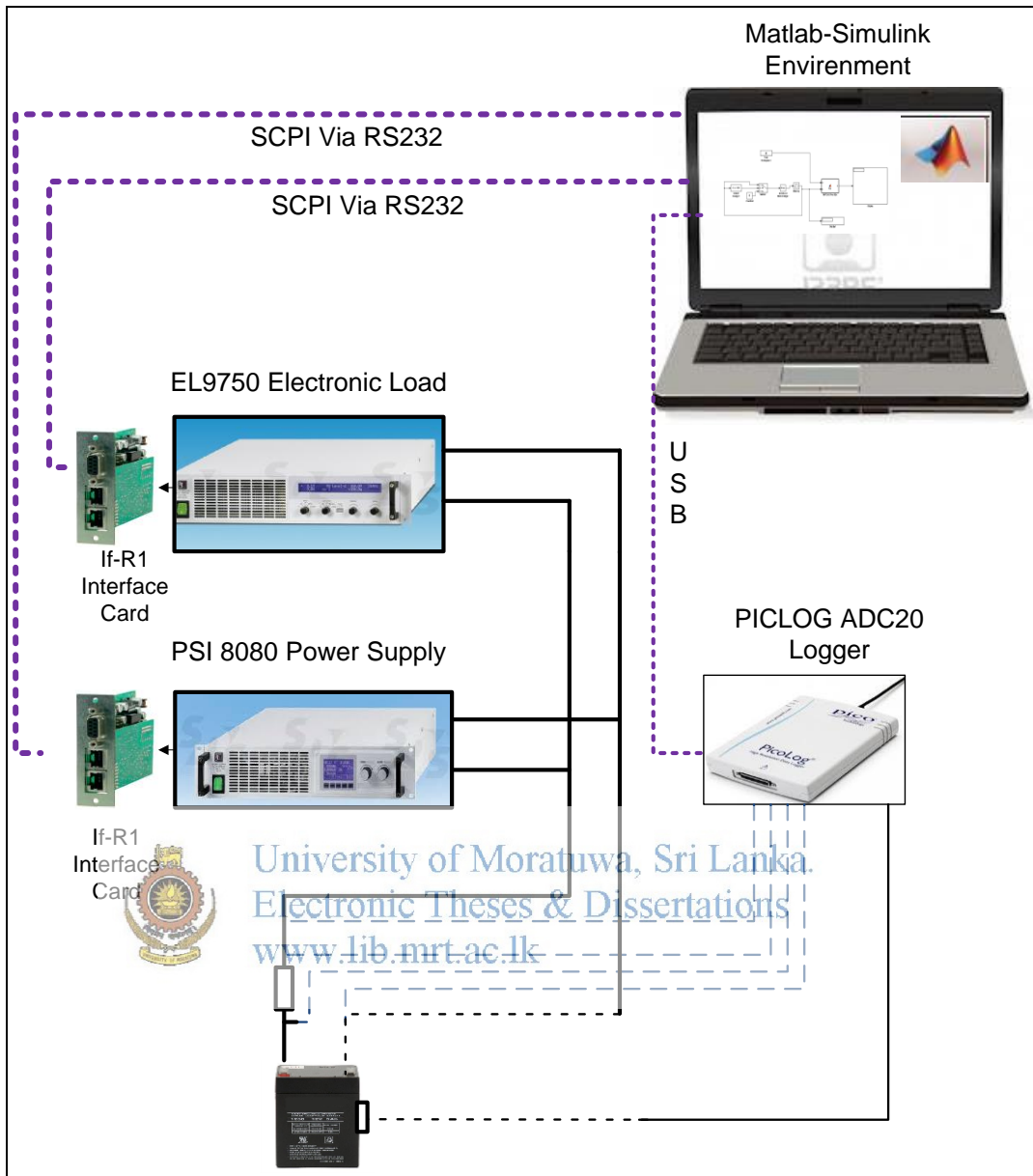


Figure 4.1: HIL Testing rig for battery monitoring and charge/discharge controlling

4.2 Voltage and current measurement.

Voltage and current is measured using three differential channels in PICO log data acquisition unit. The assignment of channels for each signal is specified in the relevant level2 S-function code in Matlab Simulink. The figure 4.2 shows the relevant connections in the measurement board and the respective channels used. Channel 1 and 2 are used for differential current measurement while channel 3 and 4 are for voltage measurement.

Voltage divider arrangement is used to step down to voltage to compatible ± 2.5 V range of data logger. This ratio ($R1/R2$) should be given as a user input for the program, as per the actual resistance values used in the circuit.

For the current sensing 0.01 Ohm resistor ($R3$) is used in the circuit. This was selected so that there will be minimum voltage drop due to this addition of a resistor in series with the circuit. The resistance of this should also be input as a user parameter and this needs to be calculated practically by trial and error since the stated value on the resistor can differ due to solder resistance at joints.

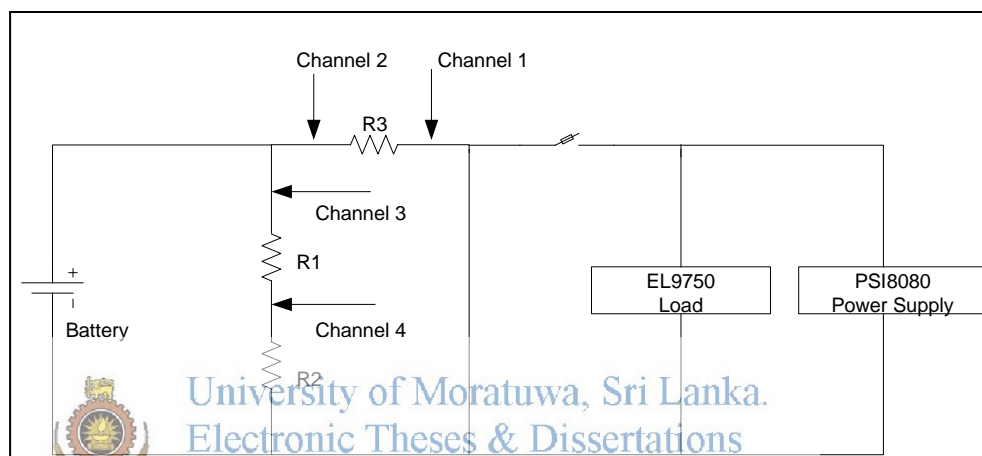


Figure 4.2: Measurement circuit diagram

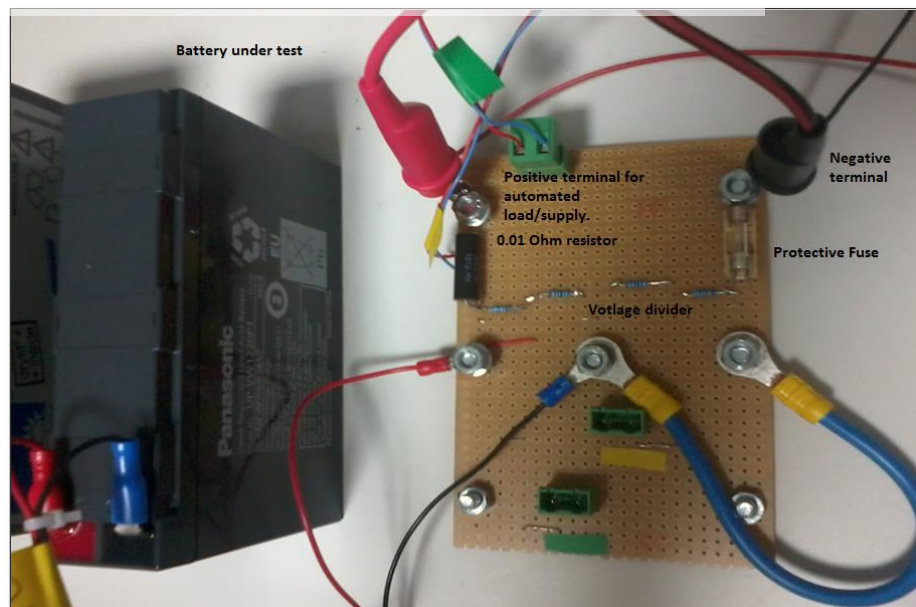


Figure 4.3: Measurement circuit media components.

4.3 Charge source - programmable remote controllable power supply(PSI8080)

PSI8080 is a microprocessor controlled laboratory power supply of series EA-PSI 8000. This allows the user to define profiles, which can be saved and archived so that the test or other applications can be reproduced. Also most importantly it provides a communication protocol (SCPI) to interface with external computer or similar device through which the test process can be automated. A dynamic profile can be transferred to PSI 8080 via this protocol in real time. An external device can be linked to the PSI8080 system via a serial port via its IF-R1 interface card. Also several numbers of same type of power supplies can be connected in a complex test setup and be controlled from a single application. Each of the devices in the configuration need to be uniquely identified by setting a node number and this can be adjusted from the device menu of PSI8080.



Figure 4.4: PSI8080 remote controllable programmable power supply

4.4 Electronic load- Programmable remote controllable electronic load(EL975)

EL9750 is a microprocessor controlled laboratory electronic load. Similar to PSI8080 electronic load is also remotely accessible and controllable via SCPI protocol. This enables the user to give a desired dynamic load profile to mimic a behavior or a load pattern. A profile can be externally fed to the electronic load and fully automate the testing.



Figure 4.5: EL975 remote controllable programmable electronic load

4.5 Protection of the system.

Different protection measures are implemented for the over voltage and over current protection of the system. First line of protection is done from the program during execution by continuously monitoring for the over voltage. But over current protection is not provided from the program but instead a quick blow fuse is deployed for this in the measurement circuit.

Second line of protection is provided via the PSI 8080 menu, supervising section. Safe limits of voltage and current is specified here to prevent any abnormality, in which case the device self-protect itself giving an alarm.

4.6 Simulink program.

The integration and communication of the devices is done in a simulink model as shown in figure 4.6. All specific communication handling and timing ect is implemented in level-2 s-functions inside triggered sub systems. The program has two main segments divided as to 'Load profile setter' and 'PICO measurements'. Purpose of 'Load profile setter segment' is to set the current and voltage settings to the PSI8080 power supply and EL9750 electronics load.

The triggered subsystems are used to mimic the parallel processing so that the 'supply/load profile setter' subsystem and 'PICO measurements' subsystem can work are two independent processes driven by two different clocks. Detailed description of different clocks is described in the sections 4.6 and 4.7.

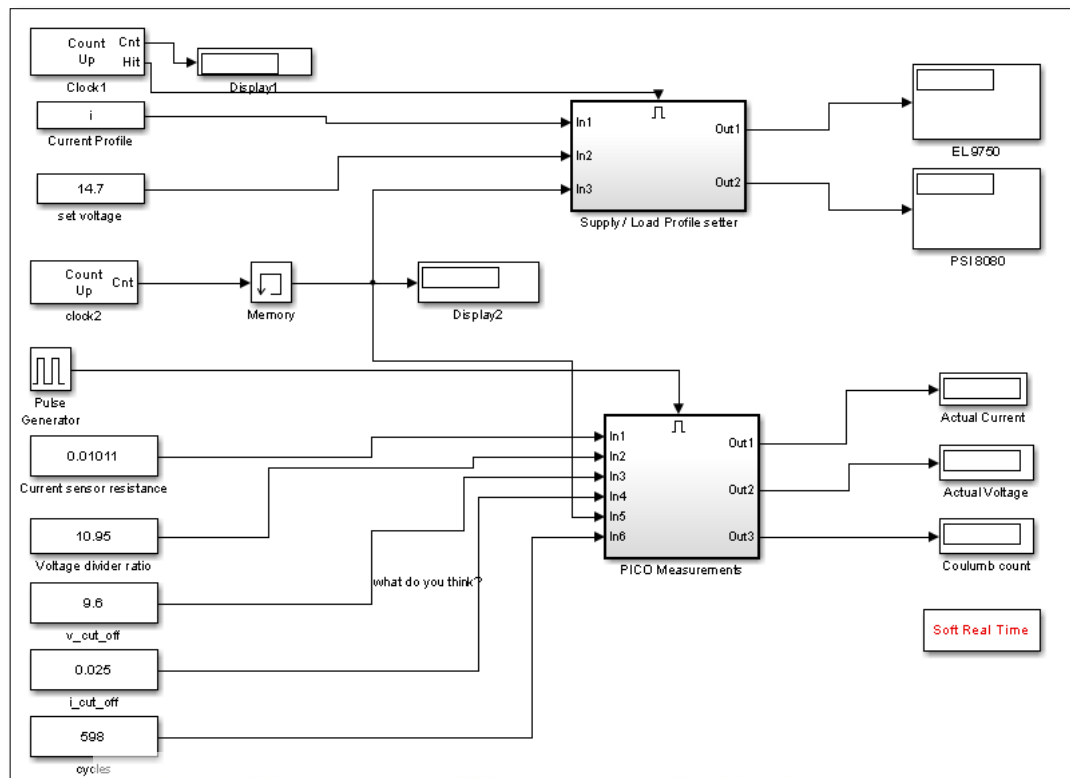


Figure 4.6: Simulink program

4.7 Load profile setter sub system.

The code is written in level 2 s-functions and embedded inside a triggered subsystem. This subsystem consists of all the communication handling with the PSI8080 and EL9750. All communications between these two devices happen via Serial physical media and via SCPI (Standard Commands for Programmable Instruments) protocol. Different function calls are implemented inside the level 2 s-function for functions such as set current value, get actual current value, put device to remote mode, put device to on state ect. Detailed function implementation, source code, can be found in Annex 01 of the document.

Basic telegram structure of a packet that is used to either transmit or receive data via IF-R1 interface is as shown bellow.

SD+DN+OBJ+DATA+CS.

SD – Start delimiter which determines how to handle the telegram further more. First 4 bit of SD specifies the data length of the telegram. 5th Bit defines the direction of communication as to whether it is from device to controller or wise-versa.

DN – Device node is the unique number allocated for devices in the whole system where more than one electronic power supply or load devices are there. Control program address the devices uniquely using the device node.

OBJ- Communication objects or functions are the different type of commands to change voltages, read parameters ect. The list of objects is found in the IF-R1 interface card user manual.

DATA- Data field can be 1-16 bytes long.

CS- check sum is always located at the end of the telegram. It is built by the simple addition of all bytes of the program. The check sum is 2 bytes long. This field is used to transfer command value or parameter value between the device and the controller.

And example telegram to query actual voltage, current and power will look like this once it is constructed inside the program.

“55 01 47 00 9D”

And the answer to the telegram would look like bellow if it is returned with out and error,

“85 01 47 64 00 1E 00 50 00 01 9F”

4.7.1 Communication with Electronic Load and Power Supply.

Communication with EL and PSI is handled in the subsystem ‘Load profile setter’ as explained in section 4.7. Two serial com handles are opened for the respective devices and save until the program exits. Standard windows fopen and fclose is used for transmitting the packets vice-versa. Particular details of com port parameters are specified in the initialization segment of the relevant level-2 S function code (Annex 02).

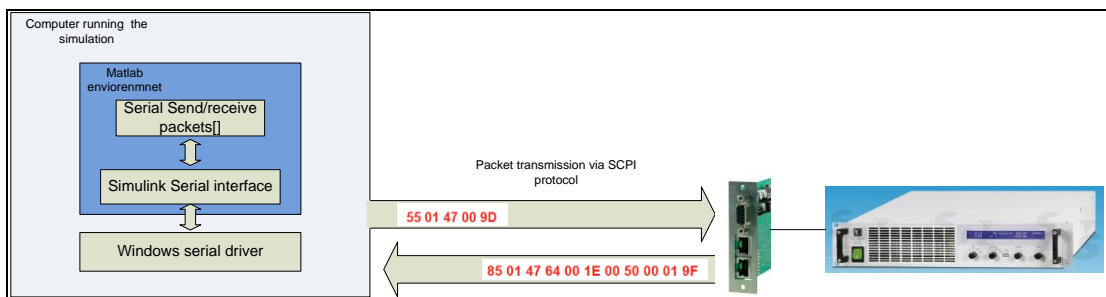


Figure 4.7: Remote communication – EL9750 and PSI8080



Figure 4.8: Elektroautomatic remote controllable electronic load and power supply rack.

4.7.2 Clock1

Clock 1 triggers 'Load profile setter' subsystem at a user desired frequency. For example user wanted to update the current every 5 second, he needs to set the maximum count of this Clock1 to 5 and hit value to 1. This will make the 'Load profile setter' invoked every 5 second interval.

4.7.3 Clock2

Clock2 keeps count of which element of the current profile (array of input current values) the program is currently pointed to. This count is used by 'Load profile setter' subsystem to load the next current value to the PSI or EL when it is triggered.

Clock2 is used by 'PICO measurements' sub system also to know which device is currently active (PSI OR EL) as per the set value of current profile at a particular instance. Clock2 is a free running up counter and its sampling rate should be set exactly equal to the maximum up count of clock1.

4.7.4 Pulse generator

This invokes the PICO measurements' sub system and the period should be set accordingly as per the user desired measurement interval.

4.7.5 Current profile

This is a 'from workspace' block which is used to give user current input profile. The user can set dynamic current profiles.

4.7.6 Set voltage

The appropriate voltage at which the batteries should be charged.



		0°C	25°C	40°C
Cycle use	4V	5.1	4.9	4.7
	6V	7.7	7.4	7.1
	8V	10.2	9.8	9.5
	12V	15.4	14.7	14.2
Trickle use	4V	4.7	4.6	4.5
	6V	7.1	6.8	6.7
	8V	9.4	9.1	8.9
	12V	14.1	13.7	13.4

Table 4.1: Charging voltages for different batteries at different ambient temperatures. [3]

4.7.7 Current sensor resistance.

This is the actual resistance of current sensing resistor.

4.7.8 Voltage divider ratio.

The multiplication factor as per the voltage divider ratio. For example if the resistance as 1 kΩ and 10 kΩ. Then the ratio will be $(10+1)/1$, which is 11.



University of Moratuwa, Sri Lanka.
Electronic Theses & Dissertations
www.lib.mrt.ac.lk

4.7.9 $V_{cut\ off}$

The safe voltage cut off level to prevent the battery from over discharging as per the manufacture. This is the second method of protection for the test setup to prevent any damages to test setup.

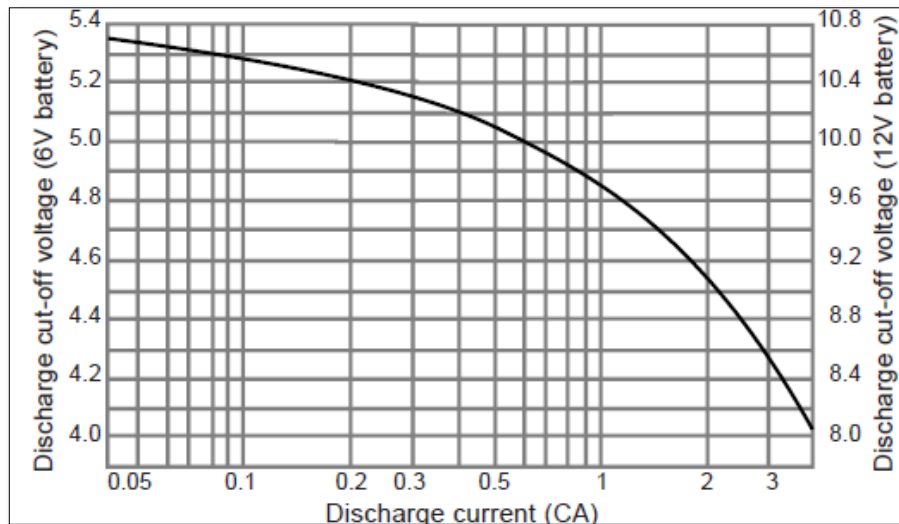


Figure 4.7:Cut off voltage for batteries against the charging current. [3]

4.7.10 I_cut_of

The safe current cut off level to prevent the battery from over charging as per the manufacture.

4.7.11 Cycles

No of cycles in multiples of the frequency of Clock2. This will stop the PSI and EL after specified number of cycles.



University of Moratuwa, Sri Lanka.
Electronic Theses & Dissertations
www.lib.mrt.ac.lk

4.7.12 Soft Real Time

This block written is C++ code synchronized the simulation clock with the real time clock of the computer. This block is used to reduce the speed of a Simulink model so that it can be observed running in real time with real external hardware.

4.8 PICO measurements sub system.

This sub system consists of all the communication handling with ADC-20 data acquisition unit. The manufacturer has provided a dynamic link library(DLL) file which were accessed by standard dll access support functions in matlab. Detailed implementation of the block can be found in the Annex 02, source code.

4.8.1 Communication with ADC-20 Data logger

The communication with PICO log is established by accessing and calling the functions implemented in PicoHRDL.dll file supplied by the PICOLOG. The correct DLL need to be selected depending on the operating system that is used. It is required to have PicoHRDL.dll renamed to HRDL.dll. HRDL.dll. and HRDL.h should be copied to the work path directory since the matlab is looking for any library file in this location. . Detailed process of initialization and data access is specified in the initialization segment and output segment of the relevant level2 s-function code. (Annex 02)

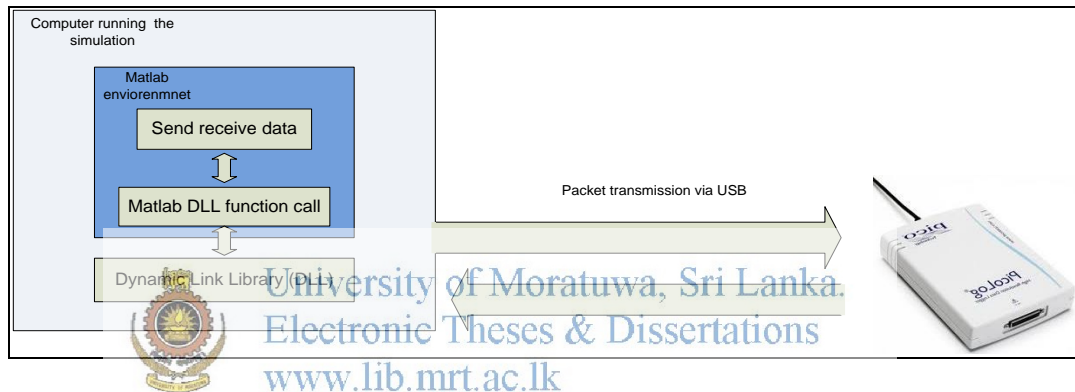


Figure 4.8: PicoLog High Resolution Data Logger ADC-20 and Terminal Board



Figure 4.9: PicoLog High Resolution Data Logger hardware

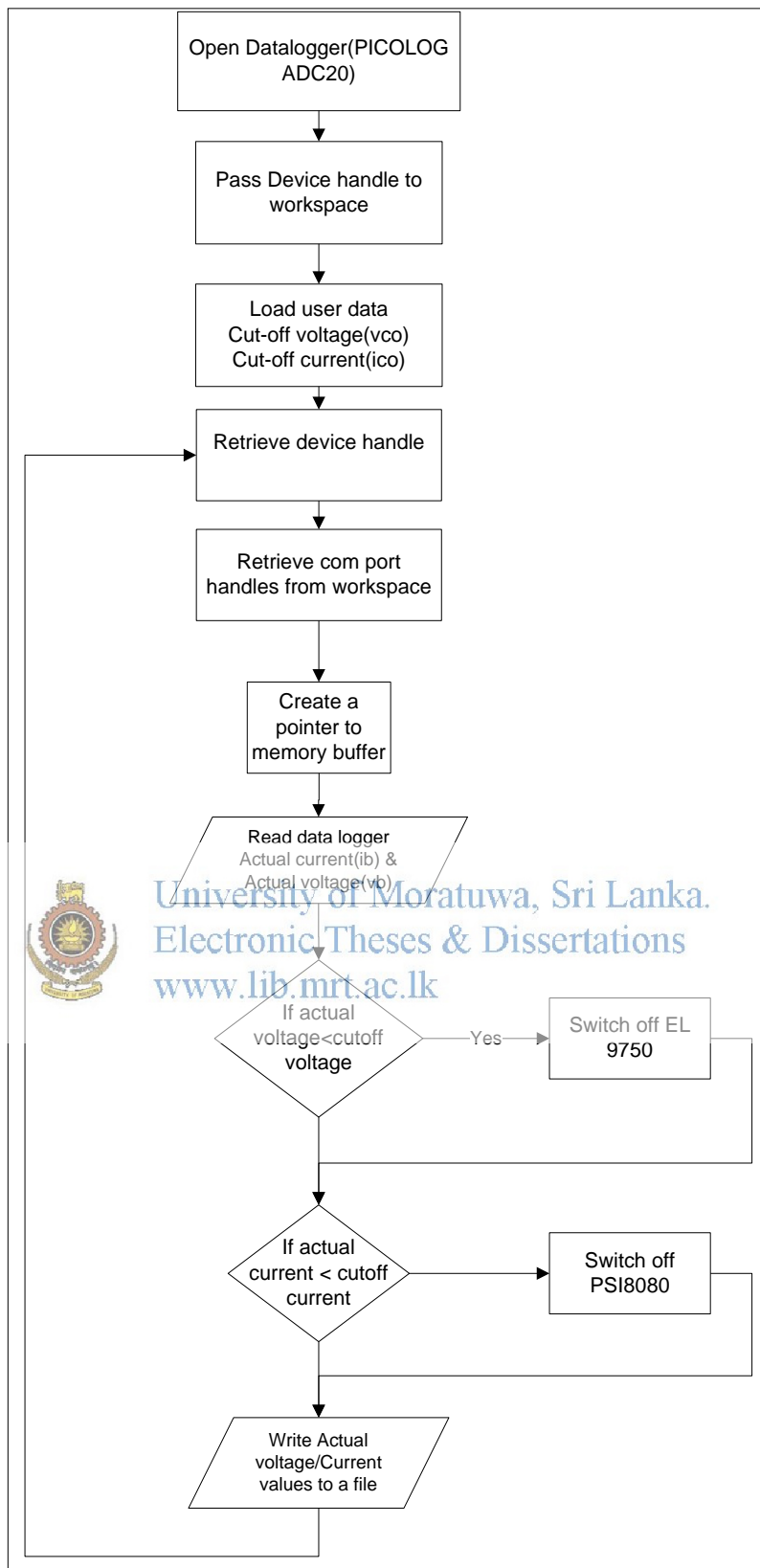


Figure 4.10: Program flow chart- PICO measurements

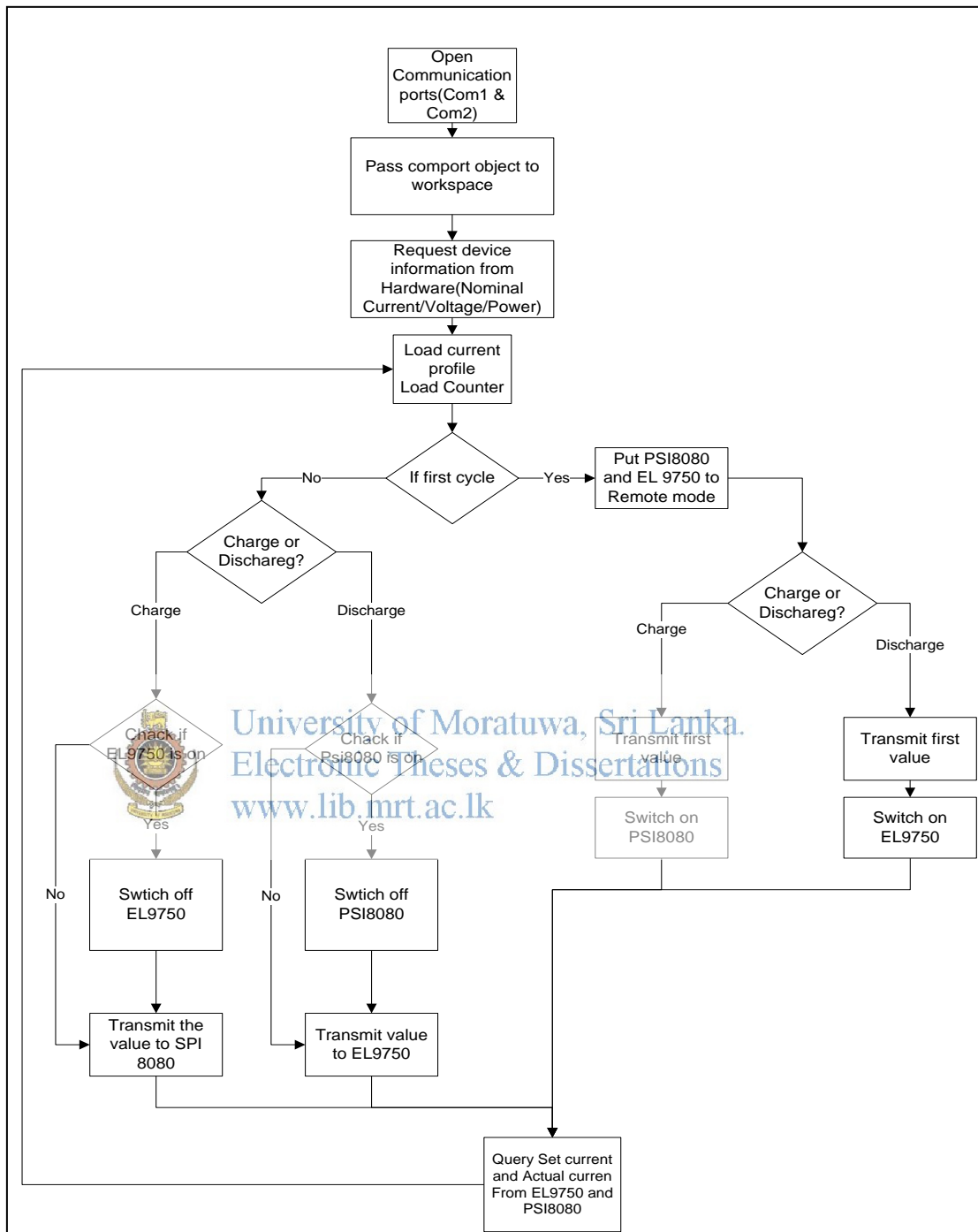


Figure 4.11 Flow diagram of Load profile setter sub system

4.8 Standard charge – discharge monitor setup with HIOKI recorder.

The second test setup was arranged to monitor several batteries and record for longer durations and high precision with HIOKI 8860 high speed waveform monitoring and recording device. This method provided a easy means of testing batteries for longer durations and acquire data in a soft format which can be easily imported to Microsoft excel.

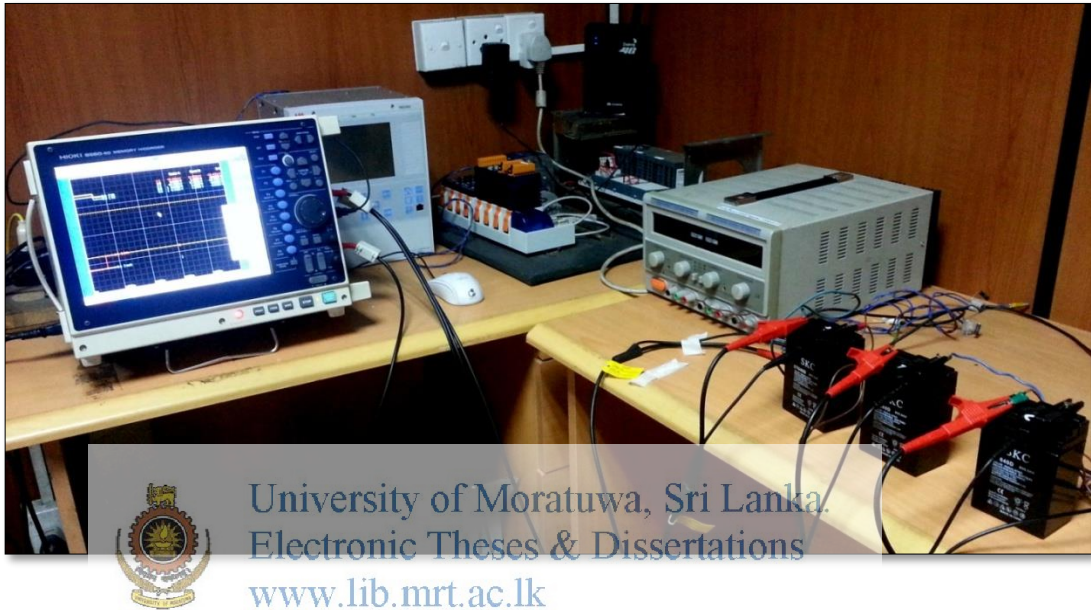


Figure 4.12: Hardware arrangement of charge-discharge monitor with HIOKI 8860 device

MODIFIED THEVENIN'S MODEL BASED ESTIMATION OF SOC

All the state of charge estimation methods discussed in chapter 3 have their own drawbacks or impracticalities in devising a method for estimating state of charge of batteries in a series array in an application of small scale solar power storage. The idea of the thesis is to experiment and recommend an accurate method to prevent over discharge of batteries in an installation. To decide or predict the discharge cut-off point, one accurate method would be to estimate the state of charge of batteries precisely during the discharge process. As discussed in chapter 3 a lot of research efforts have gone into producing different methods of estimation, but not all of them are applicable in the context of this thesis. On the other hand the proposed method shall be easy to implement in a domestic installation with minimum amount of external measurement parameters.

The modified Thevenin's Circuit (figure 5.1) developed for estimating the open circuit voltage, based on the paper "Estimating the State of Charge of a Battery" by John Chiasson and Baskar Vairamohan[1], published in "Transactions on Control Systems Technology" is used here to test its applicability to more than one battery in a series configuration. The control theory approach described here is strongly based on [1]. The model described in section 3.5 was used for modeling the battery's behavior as it accounts for energy losses in all forms as well as the transient behavior of the internal current of the battery.

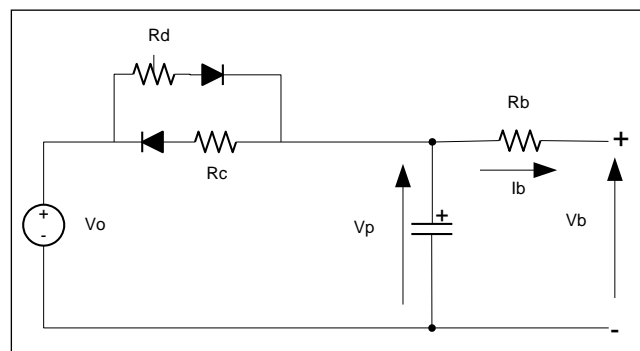


Figure 5.1: Modified Thevenin's equivalent circuit model.[1]

- Resistance R_c and R_d , for accounting for electrical and non-electrical losses during charging and discharging cases.
- Resistance R_b , for accounting for internal resistance.
- Capacitor C , for accounting for transient current conditions.

5.1 Basic equations for discharging.

By applying Kirchhoff's Current Law, considering discharging case,

$$\dot{V}_p = -\frac{V_p}{R_d \cdot C} + \frac{V_o}{R_d \cdot C} - \frac{I_b}{C} \quad \text{And} \quad (5.1)$$

$$V_b = V_p - I_b R_b \quad (5.2)$$

5.2 Construct State Space model.

State space variables were intuitively identified to represent the system parameters as in equations (5.3).

$$X_1 = V_p$$

$$X_2 = \frac{1}{R_d \cdot C}$$

$$X_3 = \frac{V_{oc}}{R_d \cdot C}$$

$$X_4 = \frac{1}{C} \quad (5.3)$$

$$X_5 = R_b$$

5.3 Identify the final objective.

It is of the interest to find V_{oc} from the knowledge of terminal voltage V_b and current I_b which are the only measured parameters of the system. Idea here is to use the relationship between settled open circuit voltage and the SOC to predict SOC real time.

Where from above state variables,

$$V_{oc} = \frac{x_3}{x_2} \quad (5.4)$$

5.4 Conversion of state space model to linear time varying model.

By converting the above (5.1) and (5.2) by applying the state variables identified in section 5.2, bellow non-linear time varying state space model was obtained,

$$\begin{aligned} \dot{x}_1 &= -x_1 x_2 + x_3 - I_b(t) x_4 \\ \dot{x}_2 &= 0 \\ \dot{x}_3 &= 0 \\ \dot{x}_4 &= 0 \\ \dot{x}_5 &= 0 \\ V_b &= x_1 - I_b(t) x_5 \end{aligned} \quad (5.5)$$

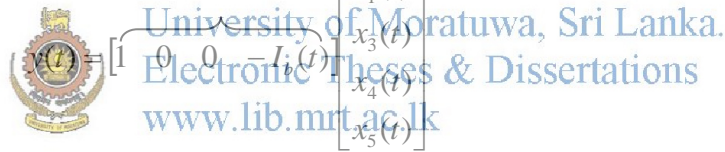


University of Moratuwa, Sri Lanka.
Electronic Theses & Dissertations
www.lib.mrt.ac.lk

5.5 Converting nonlinear state space system to linear time varying system.

Assuming initial state of x_2 , that is x_{20} is known, the above nonlinear state space modal was viewed as a linear time varying system, and expressed in matrix form. A value for x_{20} which is $1/Rd.C$ was approximated for the initial state. Results of tests carried out to find the impact of this initial estimate it in section 5.11.

$$\frac{d}{dt} \begin{bmatrix} x_1(t) \\ x_3(t) \\ x_4(t) \\ x_5(t) \end{bmatrix} = \begin{matrix} \text{A} \\ \overbrace{\begin{bmatrix} -x_{20} & 1 & -I_b(t) & 0 \\ 0 & 0 & 0 & 0 \\ 0 & 0 & 0 & 0 \\ 0 & 0 & 0 & 0 \end{bmatrix}} \end{matrix} \begin{bmatrix} x_1(t) \\ x_3(t) \\ x_4(t) \\ x_5(t) \end{bmatrix} \quad (5.6)$$

$$\begin{matrix} \text{C} \\ \begin{bmatrix} 1 & 0 & 0 & -I_b(t) \end{bmatrix} \end{matrix} \begin{bmatrix} x_1(t) \\ x_3(t) \\ x_4(t) \\ x_5(t) \end{bmatrix} \quad (5.7)$$


5.6 Solution for the linear time varying system.

Above (5.6) and (5.7) is in the familiar form of,

State differential equation $\dot{x} = Ax + Bu$

and

Output equation $y = Cx + Du$

Considering the a first order differential equation of the form $\dot{x} = ax + bu$

Where x and u are scalar functions of time, if the Laplace transform is obtained

$$sX(s) - x(0) = aX(s) + bU(s)$$

$$\text{Therefore } X(s) = \frac{x(0)}{s-a} + \frac{b}{s-a} U(s)$$

If the matrix format of the same is considered in similar manner it can be expressed as,

$$X(s) = [sI - A]^{-1}x(0) + [sI - A]^{-1}BU(s) \quad (5.8)$$

where

$$A = \begin{bmatrix} -x_{20} & 1 & -I_b(t) & 0 \\ 0 & 0 & 0 & 0 \\ 0 & 0 & 0 & 0 \\ 0 & 0 & 0 & 0 \end{bmatrix}$$

$$C = [1 \quad 0 \quad 0 \quad -I_b(t)]$$

and

$[sI - A]^{-1} = \varphi(s)$ which is the Laplace transform of the state transition matrix, $\varphi(t)$

$$L^{-1} \left[\frac{1}{s-a} \right] = e^{at} = \varphi(t)$$

where,

$$\varphi(s) = L[\varphi(t)] = L[e^{at}] = [sI - A]^{-1}$$

Hence $\varphi(s)$ is the Laplace transform of $\varphi(t)$ which is the Laplace transform of $\varphi(t) = e^{At}$, which is called the state transition matrix. (A,C) is said observable on (t_0, t_f) if any initial state $x(t_0) = x_0$ can be uniquely determined from $y(t)$. Observability gramian is hence defined as,

$$W(t_0, t_f) = \int_0^{t_f} \Phi(t)^T C^T C \Phi(t) dt \quad (5.9)$$

Then $x(t_0)$ has a unique solution for state differential equations (5.6 and 5.7) from theory, which can be expressed as,

$$x_0 = W^{-1}(t_0, t_f) \cdot \int_0^{t_f} \Phi(t)^T C^T y(t) dt \quad (5.10)$$

To find the solution it is needed to find $\varphi(t)$ while C and y(t) is already known,

$$\frac{d}{dt} \varphi(t, t_0, x_{20}) = A(t, x_{20}) \cdot \varphi(t, t_0, x_{20})$$

This is analogous to $\frac{d}{dt} e^{At} = A \cdot e^{At}$

To find $\varphi(t)$, where

$$\varphi(t) = L^{-1} [[sI - A]^{-1}]$$

by expanding the matrix and finding inverse Laplace transform,

$$L^{-1} [[sI - A]^{-1}] = \begin{bmatrix} s - x_{20} & -1 & I_b(t) & 0 \\ 0 & s & 0 & 0 \\ 0 & 0 & 1 & 0 \\ 0 & 0 & 0 & 1 \end{bmatrix}^{-1} \quad (5.11)$$

From this it is found,

$$\varphi_{11} = e^{-x_{20}(t-t_0)} \quad (5.12)$$

$$\varphi_{12} = \frac{1}{x_{20}} (1 - e^{-x_{20}(t-t_0)}) \quad (5.13)$$

$$\varphi_{13} = - \int_{t_0}^t e^{-x_{20}(t-\tau)} I_b(\tau) d\tau \quad (5.14)$$

5.7 Matlab Simulink implementation.

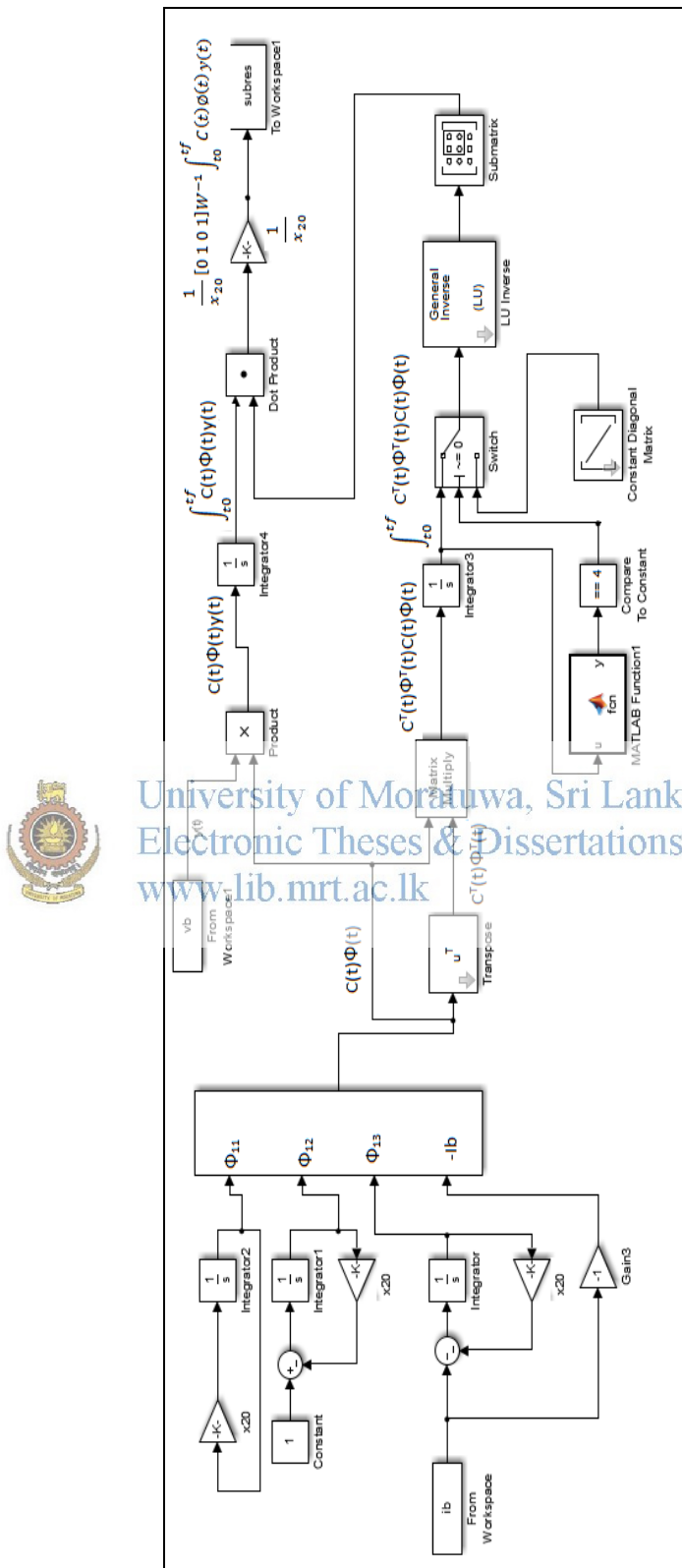


Figure 5.2: Matlab Simulink implementation of the state space model

The solution for the state space equation above was implemented in Matlab Simulink version R2013 and combined with the HIL system developed for testing. The measured inputs I_b and V_b can either be connected in real time or from a file. To work with the HIL testing setup real time measured data was input to the system.

Initially the system constructs resultant of $\Phi(t)C(t)$ which is a row matrix $[\Phi_{11}\Phi_{12}\Phi_{13} -I_b(t)]$ as shown in the figure 5.2. Then the transformation of the same is done using transpose block and these two results are multiplied and integrated to produce the observability gramian. The full rank of observability gramian means, on a given point of time the state vector can determine the output. Hence the full rank of observability gramian is checked before passing over the result to next step.

$\Phi(t)^T C(t)^T y(t)$ is separately calculated in a different branch and then integrated, to be ready for final dot product with result of observability gramian. The two inputs to the working model is I_b and V_b and only output from the system is the results generated when running the real time hardware in the loop test, synchronized with real time clock(RTC) of the PC in which the Simulink is running.

5.8  **Testing devices and arrangement.**
 University of Moratuwa, Sri Lanka.
 Education, Training & Dissertations
www.lib.mrt.ac.lk

Set of sealed lead acid batteries, which are in small capacity were used for the testing in the lab due to easy handling and to minimize the risks during tests when run for unattended longer hours. Table 5.1 shows different batteries used in the lab for experiments. Test setup was prepared as explained in Chapter 4.

Battery No	Type	Brand	Capacity	Voltage
1	VARL	ProLink	8.2 Ah	12V
2	VARL	Panasonic	6 Ah	12V
3	VARL	Exide	4 Ah	6V
4	VARL	SKC	4.2Ah	6V
5	VARL	SKC	4.2Ah	6V
6	VARL	SKC	4.2Ah	6V

Table 5.1: Batteries used for testing work.

5.9 Deriving state of charge from OCV.

As explained in section 2.8 the open OCV has a linear relationship to its residual charge. Thus the OCV at the fully charged state and fully discharged state were experimentally determined for all the batteries under test. The linear relationship was then used to derive the SOC at a given point from its OCV estimated from the calculations. For all the tests bellow, OCV of the battery was recorded manually using Fluke 87V multimeter, before and after each test, for the purpose of verification.

To arrive at the SOC at a given time t , from the OCV estimated from the modified Thevenin's model, equation (5.15) was applied.

$$SOC(t) = \frac{OCV \text{ estimated}(t) - OCV \text{ Fully discharged}}{OCV \text{ Fully charged} - OCV \text{ Fully discharged}} \times 100 \quad (5.15)$$

For comparison purpose, the same data was applied coulomb counting method to calculate the state of charge as a reference. The current going out is integrated over time to calculate the amount of discharge up to the point of interest using equation (5.16). This result is deducted from the initial SOC of the battery derived from the equation (5.17).

$$Q(\text{Discharged}) = \int_{t_0}^t Ib dt \quad (5.16)$$

$$SOC(\text{Start}) = \frac{OCV \text{ settled}(\text{Start}) - OCV \text{ Fully discharged}}{OCV \text{ Fully charged} - OCV \text{ Fully discharged}} \times 100 \quad (5.17)$$

To find the SOC at any given point the equation (5.18) is used, which subtracts the percentage of energy dissipated since start from the SOC at start point.

$$SOC(t) = SOC(\text{Start}) - \frac{Q(\text{Discharge})}{Q(\text{Fully Charged})} \quad (5.18)$$

5.10 Tests & Results

5.10.1 Comparison of SOC estimated with SOC calculated from coulomb counting.

The figure 5.3 shows the SOC estimated based on coulomb counting starting from a known initial point and SOC based on OCV estimated by using the modified Thevenin's model explained in above. Panasonic 12V,6Ah seal lead-acid battery was used in the test. Here the measured open circuit voltage at the settled state of the battery is 12.91v. OCV at fully charge state and fully discharged state were measured to be 13.04v and 11.96v.

The test was carried out by applying a varying load of sine shaped current wave form from the electronic load for 10 minutes continuously. V_b and I_b are the terminal voltage and current.

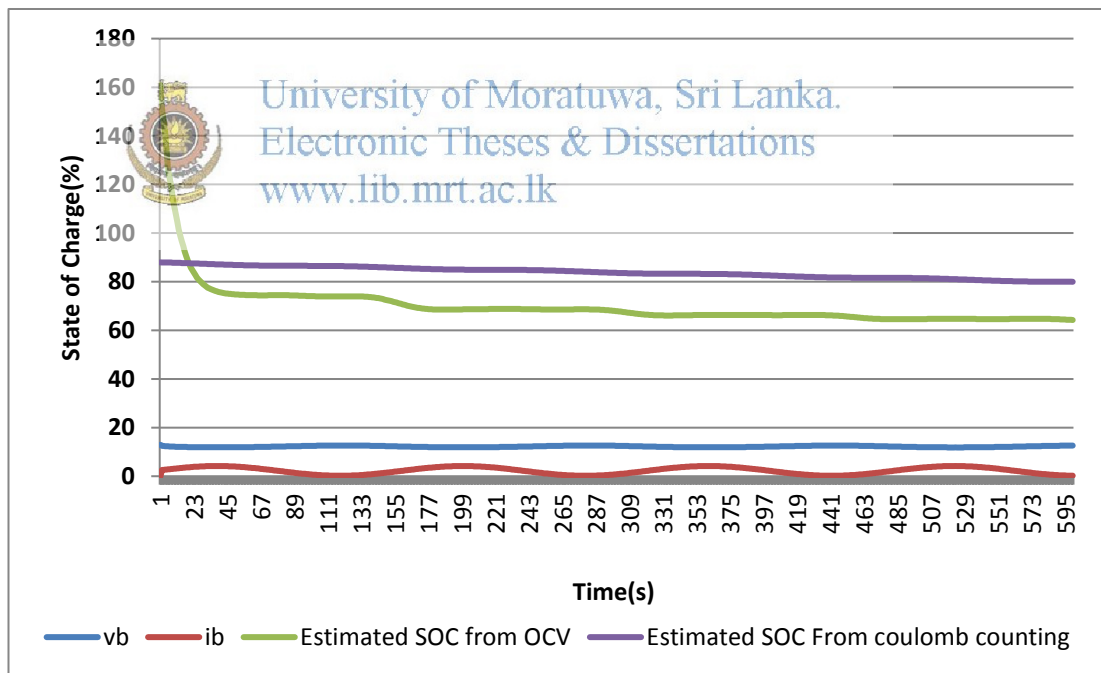


Figure 5.3: Estimation of SOC using OCV and Coulomb counting

The comparison of the SOC from OCV and coulomb counting, it was noted that the two graphs follows the same profile but there is an offset of 5%-8% from the beginning which continue until the end of the test. This can be an error due to

wrong estimation of initial state of charge. Also it was noted that during first 40 to 50 seconds the control algorithm produces an error but converges to a stable value after that.

5.10.2 Impact of x_{20} on the calculation.

In order to practically check the impact of initial estimation of X_{20} on the result of OCV calculated at any given time (After the initial correction phase is over) several practical values for x_{20} was selected and applied to the algorithm to find the solution. In here R_d was selected from 2.5 m Ω to 25 m Ω as per the common figures from manufactures datasheets at full charge. And C was selected to be 40F [1]. Hence $1/R_d.C$ can vary from 10 to 1 for the test values. Test was carried out for 4 X_{20} values in this range which produced the figure 5.4.

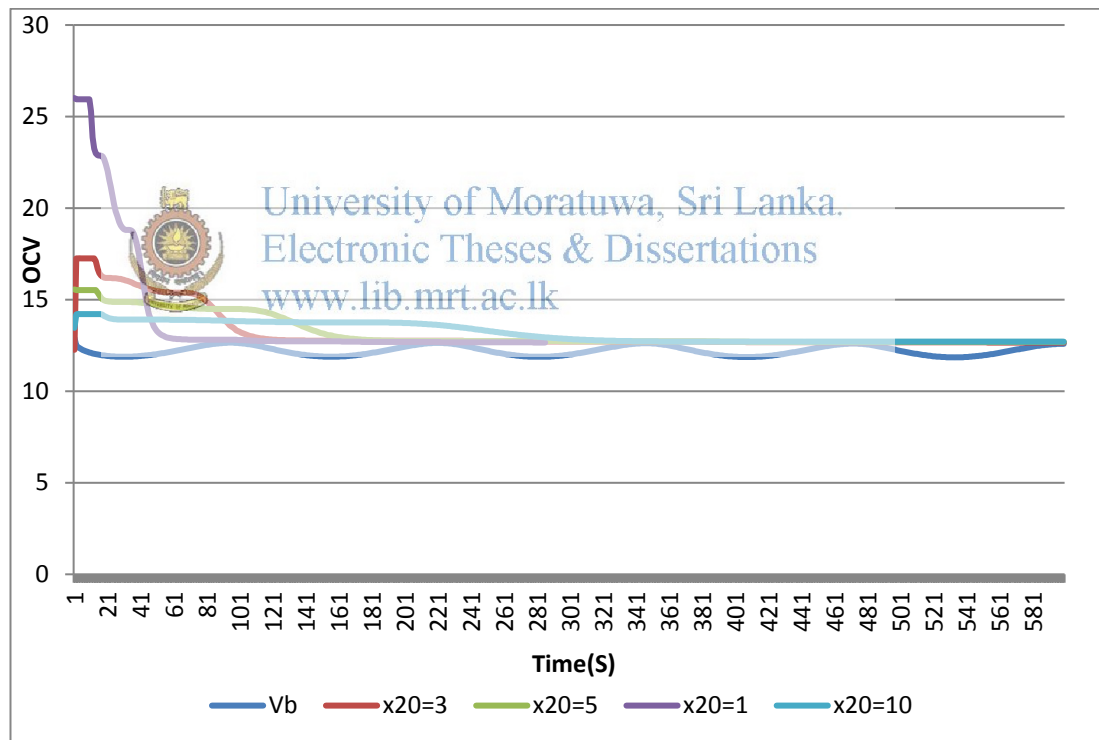


Figure 5.4: Testing of the system for different initial values of X_{20} .

For the discharging test carried out with a sine type load profile all values for the OCV converged to same value 12.68V. But the use of higher x_{20} took more time to converge to the correct value from initial correction phase.

5.10.3 Charging case

Tests were carried out on ProLink, 12V, 8.2Ah sealed lead acid battery for the charging conditions to verify the results produced from the model for open circuit voltage for a short time interval(7 minutes charge) . A voltage of 14.7V, as per the manufacturers recommendation was maintained in the power supply in constant voltage mode. The current limiter was controlled manually to change the current profile for varying the measurements. At all times it was made sure the current does not exceed the manufacturers recommended 2.7A initial current. Actual initial OCV measured at settled state was 12.74V whereas the same estimated from model is 12.98V. OCV settled after charging was measured to be 12.80V whereas the same from the estimated is 13.04V. The actual change in OCV from the initial point is 0.47% where as the estimated change in OCV is 0.46%.

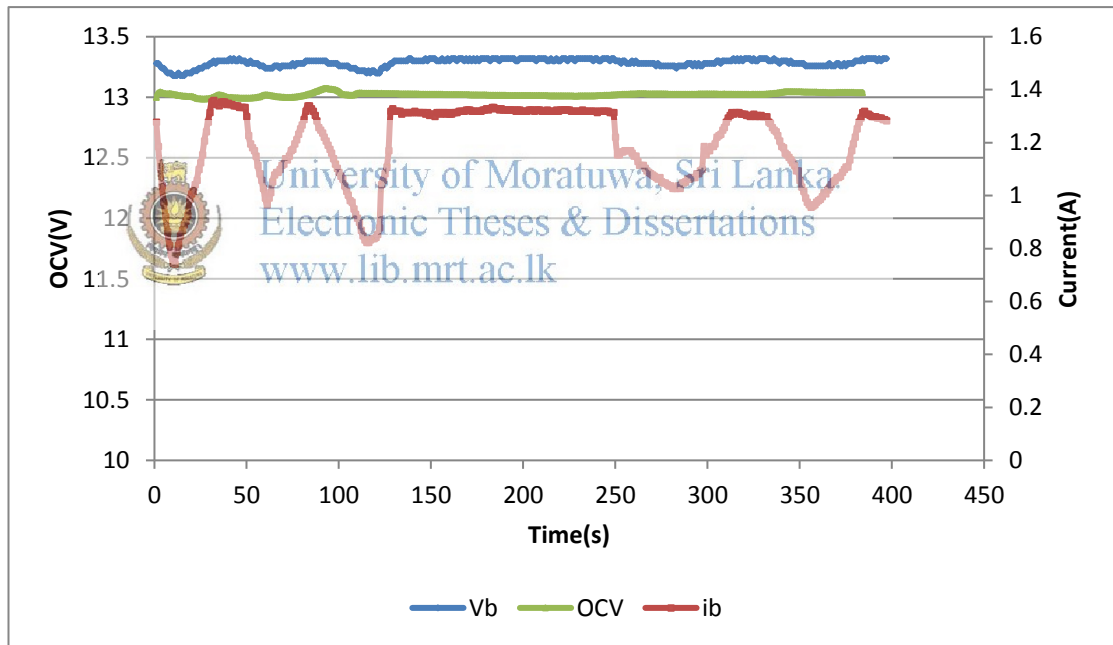


Figure 5.5: Estimation of VOC for charging case.

In charging case also it was observed that the estimated value took its first 40 seconds to converge to the correct value as it was the case with discharging. But once converged to the correct estimated value it could be observed that the voltage estimated from the algorithm is consistent and keeping bellow the charging voltage (Vb) between the two terminals of the battery.

5.10.4 Charging profile with non-charging intervals.

Figure 5.7 shows results of charging test on Exide, 6Ah battery where the electronically controlled power supply was (PSI8080) was put to the constant current mode and loaded with a profile which reaches 0 charging current in equal intervals for the test which was carried out for 7 minutes. It could clearly observe that the OVC estimated is almost touching the terminal voltage profile at times where the current becomes 0A(Which is like open circuit). This again verify that the results produced from the calculation for the OCV is accurate enough to get a good estimate of the state of charge of the battery.

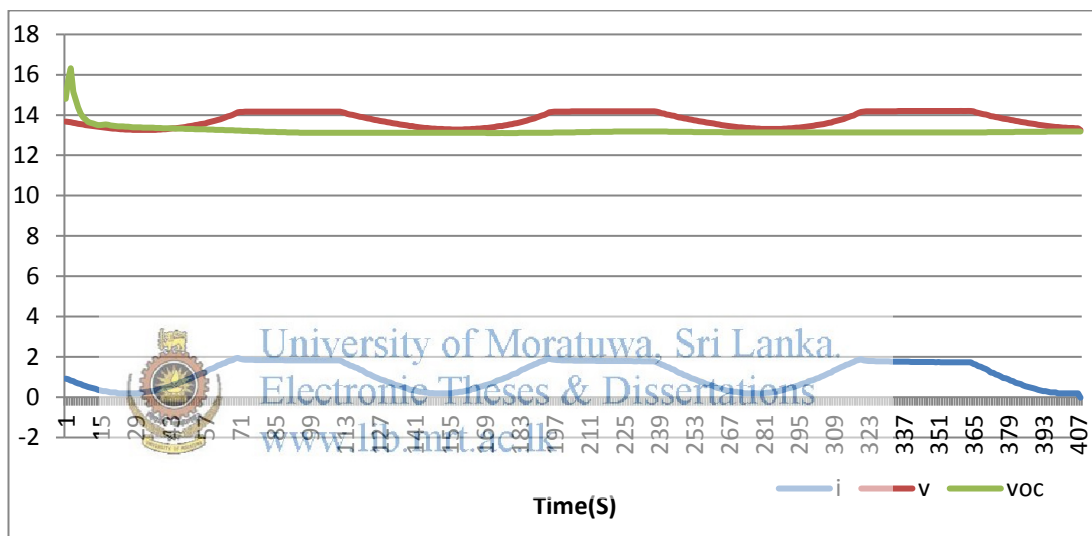


Figure 5.7: Estimation of VOC for charging case with no charging intervals.

5.10.5 Two batteries in series (Battery A & Battery C) - Discharge case.

For the better comparison purpose 2 batteries of the same make was selected. Namely battery A and Battery C, which are 4.2 Ah sealed lead-acid type from manufacturer SKC. Battery C was purposely over discharge until 1.25V/Cell at a rate of 1C until a significant reduction in effective capacity is observed.

Discharge current was automatically varied using a random current between 0.5C and 1C. After around 4 minutes, terminal voltage of battery C started to exhibit a significant drop. At the end of the test after 7 minutes discharge the estimated open circuit voltage (OCV) of battery C from the figure 5.8 is read as 5.97V.

From manufacturers data of the same battery, the residual capacity of the battery at this point is 9.5%. This indicates that the battery has already reached its unhealthy discharge range, even before reaching the specified cut-off voltage.

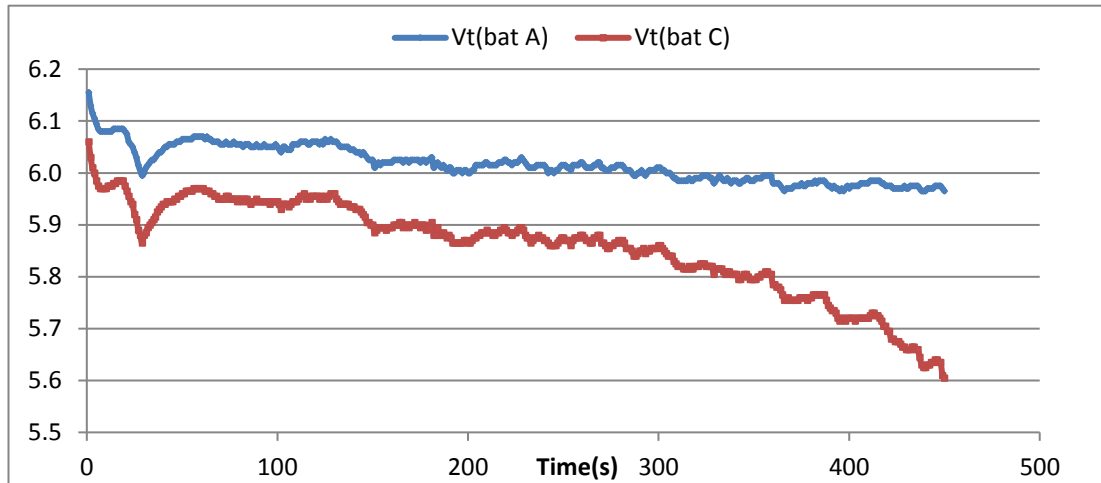


Figure 5.8: Terminal voltage of two batteries discharged in series.

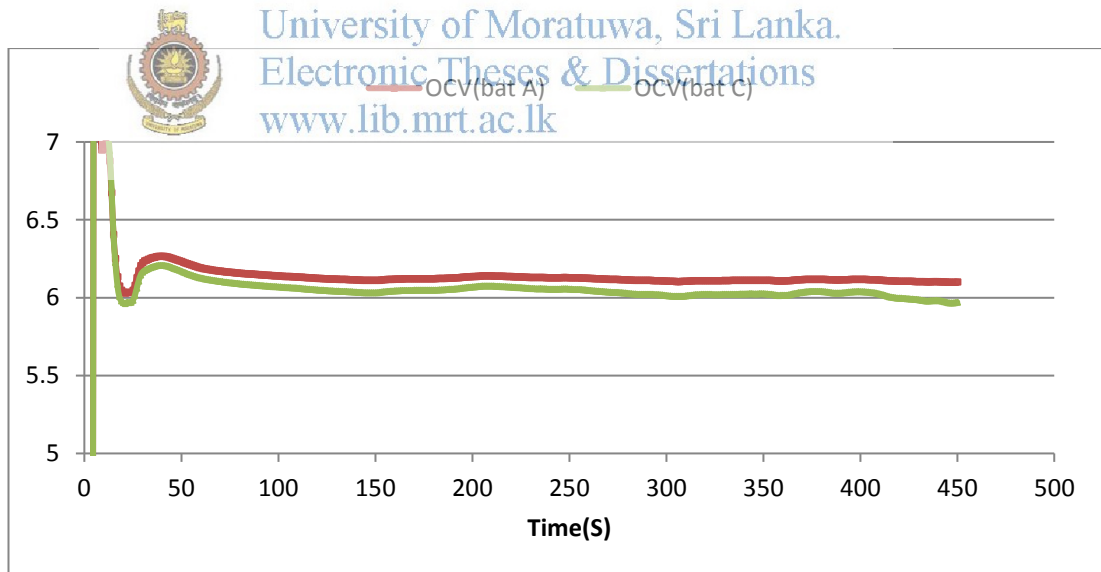


Figure 5.9: Estimated OCV of two batteries discharged in series.

PREDICTION OF END OF DISCHARGE (EOD) BASED ON VOLTAGE GRADIENT.

In the scope of this thesis, the knowledge of state of charge of a battery is of primary importance as a means of determining the end of discharge point to avoid any over discharge of batteries to prevent expediting of damages to a weaker battery. As elaborated in introduction chapter, if the EOD point is arrived based on the cut-off voltage, there is always a chance to damage a weaker battery by stressing it to its fullest capacity deliverable. Most of the market available battery controllers use a crude method of a flat cut-off voltage point to stop discharging of batteries. Higher cut-off point can under utilize the actual battery capacity while lower cut-off point can over discharge the battery. It is the focus of this chapter to devise a criterion to determine EOD without the knowledge of reserve capacity of a battery and also without stressing it to its limits. The gradient of terminal voltage during discharge process is of the interest here. It was observed from the discharge curves that the terminal voltage takes a sharp bend at around its last 5-10% of residual charge.

Discharge Current	C-Rate	Discharge Time	End of Discharge
0.5A	0.05C	20h	1.75V
0.1A	0.1C	10h	1.75V
2A	0.2C	5h	1.70V
2.8A	0.28C	3h	1.64V
6A	0.6C	1h	1.55V
10A	1C	0.5h	1.40V

Table 6.1: Typical End of Discharge voltages of 10Ah Lead Acid Battery

6.1 Battery cut-off voltage in a series of batteries.

For the tests explained below 4.5 Ah 6V Seal Lead Acid batteries of same brand and same condition were selected. Batteries were named A, B and C for the ease of referring to them in explanation and comparison. Battery C was subjected to several deep discharge cycles at 3C until it exhibits significant loss in effective capacity. To confirm each battery's true effective capacity charge-discharge tests were carried out separately.

Battery	Start Open Circuit Voltage	End Open Circuit Voltage	Energy discharged at 20hr rate	Effective Capacity
A	6.54	6.28	4.12Ah	91.55%
B	6.54	6.29	4.11Ah	91.33%
C	6.48	6.21	1.88Ah	41.77%

Table 6.2: Comparison of batteries under test.

Above confirms that the batteries A and B are of the same condition where as battery C is having significantly low effective capacity compared to A and B.

6.1.1 Batteries in series discharge at 0.25C.

3 Batteries specified in table 6.2 is used for this test after a full charge, which was arranged in series configuration. At the discharge rate of 0.25C the cut-off voltage for these batteries is selected as 5.1V. The voltages and current through the battery string was monitored until one of the battery reach the cut-off level. After around 75th minute the battery C started to exhibit a rapid drop in terminal voltage which is the knee point of discharge. It reached the cutoff voltage in another 5 minutes time. Battery A & B voltage levels remained almost consistent. This observation reveals that near the end off discharge point the terminal voltage of battery start to show a significant drop during discharge.

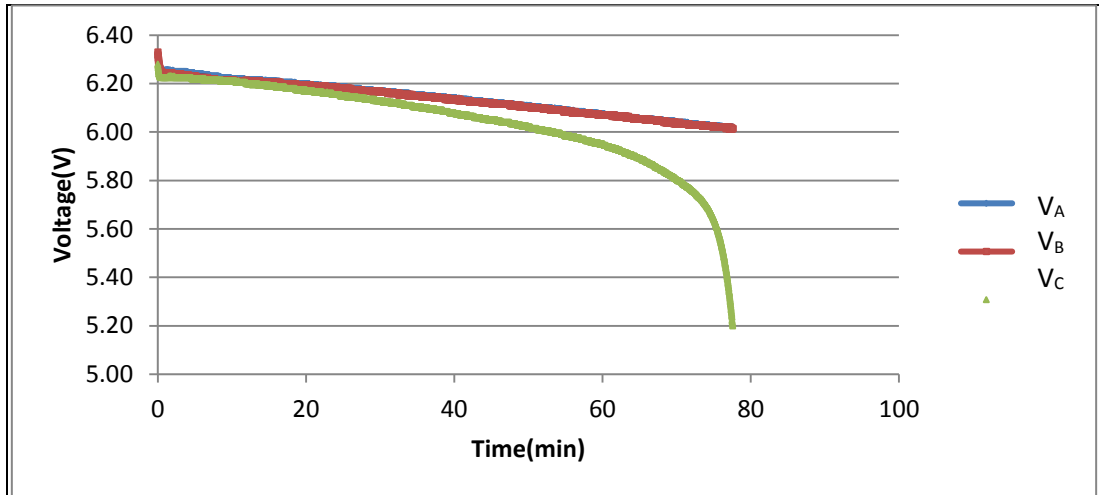


Figure 6.1: Battery A,B & C under 0.25C discharge.

6.1.2 Batteries in series discharge at 0.5C.

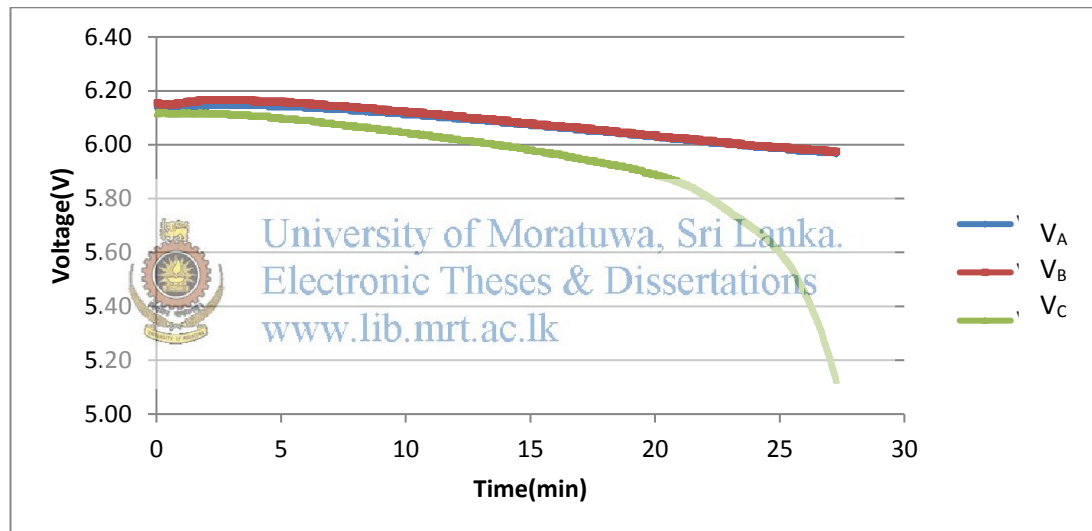


Figure 6.2: Battery A,B & C under 0.5C discharge.

Same batteries in table 6.2 after a full charge was used for this test. The same test was carried out at the discharge rate of 0.5C and the cut-off voltage was selected as 5.0V. The voltages and current through the battery string is monitored until one of the battery reach the cut-off level. After around 25th minute the battery C started to exhibit the knee point of discharge. And reached the cut-off point in another 3 minutes time while battery A & B voltage levels remained almost consistent. During this test at 0.5C, battery reached cut-off point significantly faster than in case of 0.25C.

6.1.3 Batteries in series discharge at 1 C.

All batteries were fully charged and same test was done as in section 6.1.1 and 6.1.2 at the discharge rate of 1C. corresponding cut-off voltage for these batteries were selected as 4.9V. The voltages and current through the battery string is monitored until one of the battery reach the cut-off level. After around 9th minute the battery C started to exhibit the knee point of discharge. And reached the cut-off voltage in another 2 minutes time. Battery A & B voltage levels remained almost consistent.

The comparison of figures 6.1,6.2 and 6.3 clearly indicate that the weaker battery deviate from the rest of the good batteries at one point during discharge. Identification of this knee point before the weaker battery reaches its cut-off point can save it from being stressed to its maximum capacity and its effective life. Where discharge process continues disregarding the terminal voltage of the weaker battery, it can stress it further eventually making it fail within few cycles. Section 6.2 looks at how much capacity is extractable from the battery bank after the weakest battery in the string reach its knee voltage point.

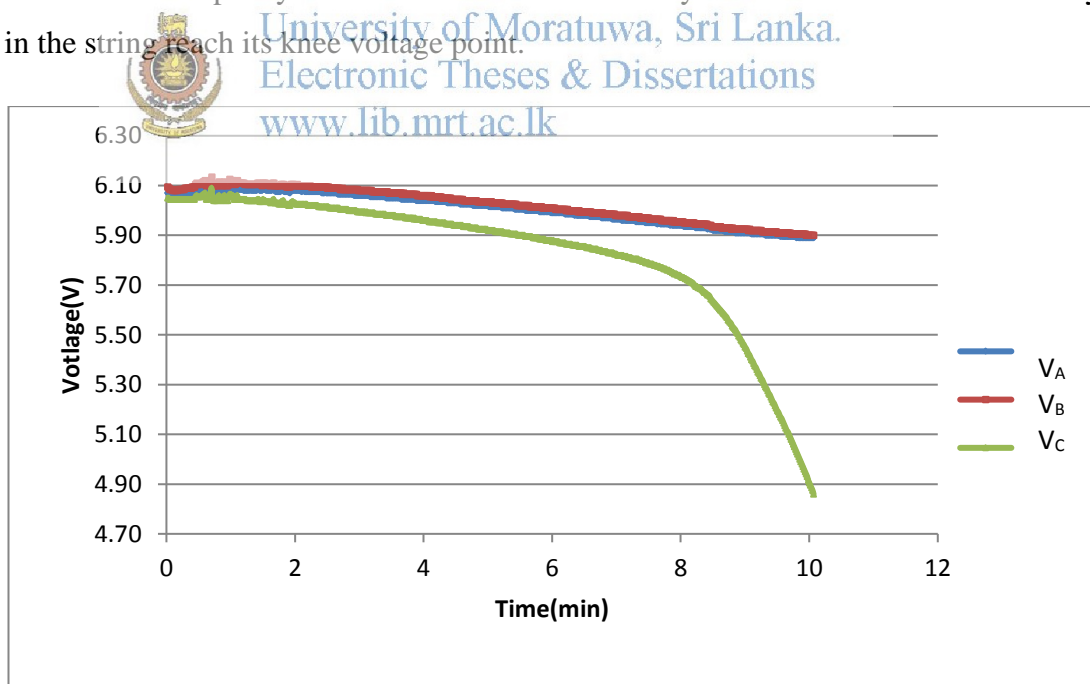


Figure 6.3: Battery A,B & C under 1C discharge.

6.2 Remaining capacity in the battery after knee point is reached.

Figure 6.4 illustrates discharge of the weak battery (Battery C) subjected to discharge at different rates from 0.25C to 1C. The cut-off voltage is reached only few minutes after the reaching of knee point voltage after which the terminal voltage rapidly drops. The remaining capacity that can be extracted after the battery reaches the knee point is of the interest here. And this is the total energy that will be extracted from the string if the discharge is further continued until the weakest battery reaches its cutoff voltage.

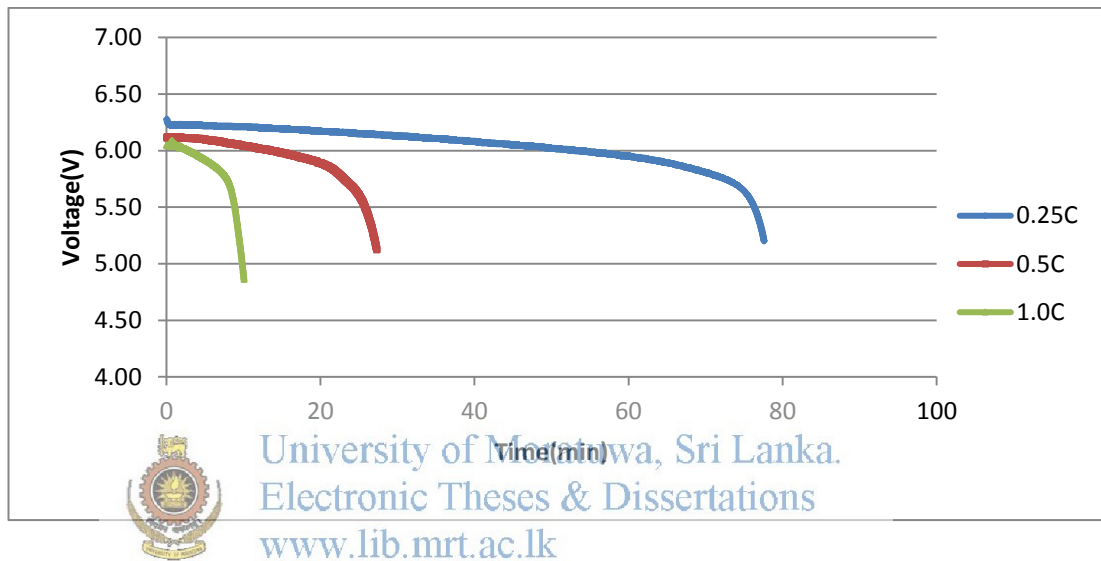


Figure 6.4: Battery discharged at different rates until respective safe cut-off levels

Table 6.3 summarizes and compare the percentage of unrecoverable energy for from the battery bank for each test under different discharge rates, had the discharge stopped at the knee point, rather than the voltage cut-off point. It is evident from the test that the percentage of energy unrecovered at lower rate of discharge is smaller than the higher rate of discharge which vary from 5%-15% range.

Rate	0.25C	0.5C	1.0C
Knee time(sec)	4421	1498	465
Cut-off time(sec)	4655	1607	604
Energy unrecovered	0.2031	0.2443	0.3375
Total Energy recovered	4.1785	2.9934	2.2242
% energy unrecovered	4.85	8.16	15.17

Table 6.3: Percentage of unrecovered energy at different discharge rates.

6.3 The rate of change of voltage drop to estimate the new knee voltage cut-off point.

In conventional battery controls the under-voltage cut-off point was specified roughly with many inherent drawbacks. The under-voltage cut-off points vary from battery to battery depending on its discharge rate and ambient temperature. Also stressing a battery to its under voltage cut-off point always sacrifices its useful life(effective capacity). Small error in specifying this point can lead to a death of a battery there by whole string of batteries. But if the end of discharge (EOD) point can be determined earlier, before reaching actual voltage cutoff point, it can save the cycle life of battery bank, on the compromise of some unrecovered energy. To determine the voltage knee point the gradient of the terminal voltage was obtained as shown in the figure 6.5, 6.6 and 6.7 for different rates of discharge using the same battery after full charge.

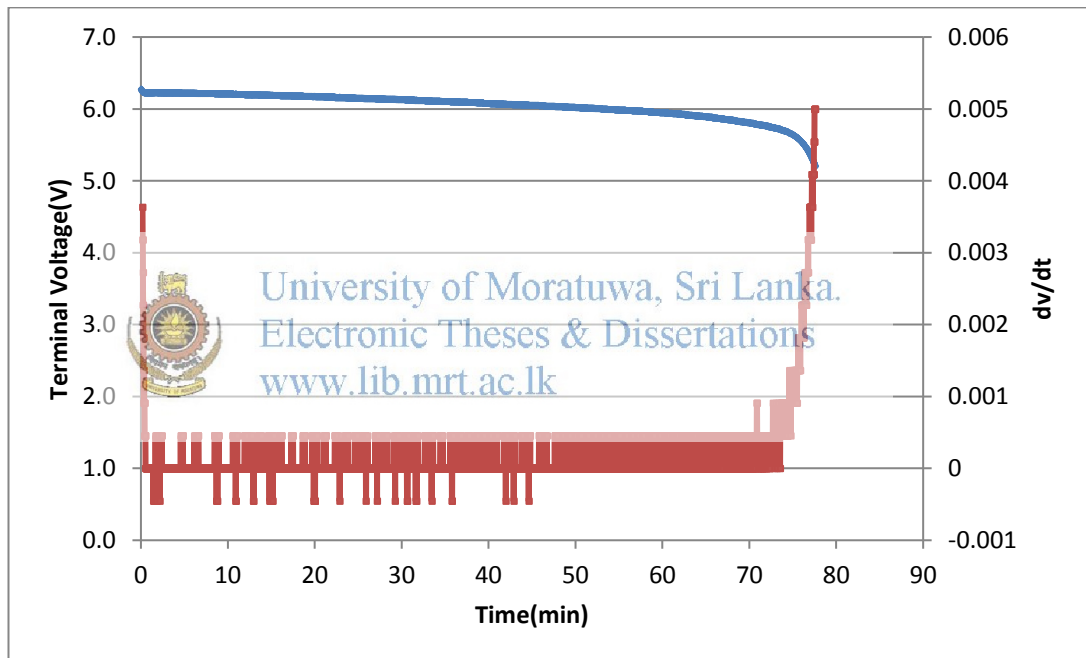


Figure 6.5 : Terminal voltage against rate of change of Terminal voltage at 0.25C

It is evident from the figures 6.5 to 6.7 that the trend of rate of change of terminal voltage takes a steep rise after reaching the knee point. Hence the discharge can be stopped by identifying this point rather than waiting for the battery to reach the actual voltage cut-off point. Figures 6.6 and 6.7 also illustrate the same behavior of the same battery at different discharge rates.

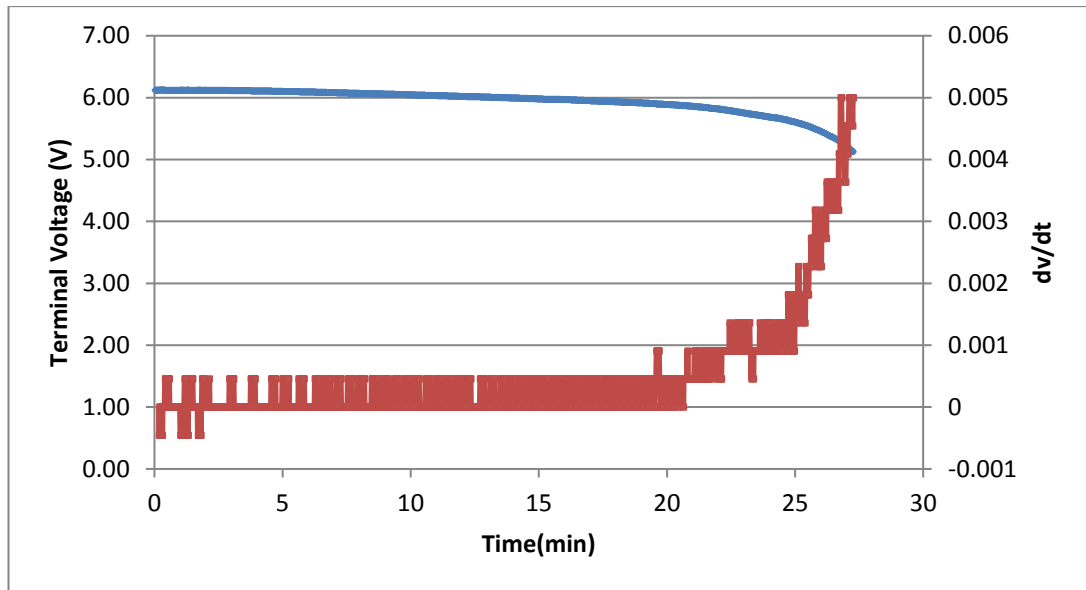


Figure 6.6: Terminal voltage against rate of change of Terminal voltage at 0.5C

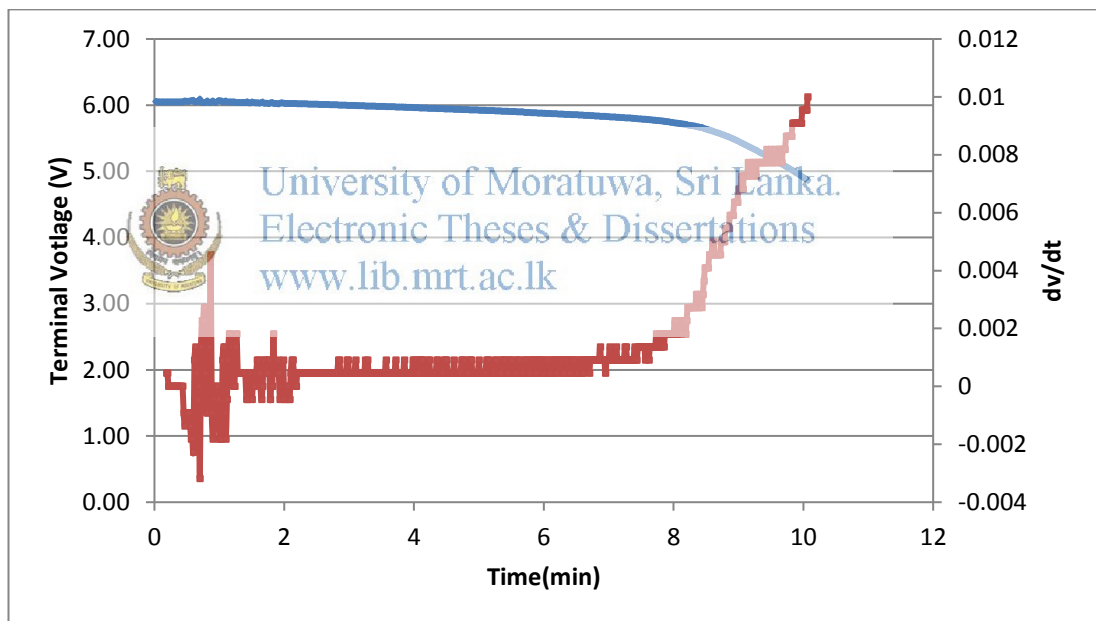


Figure 6.7 : Terminal voltage against rate of change of Terminal voltage at 1C

As per the figures 6.5,6.6,6.7 around the voltage knee point during all 3 discharge rates the gradient of rate of change of terminal voltage also start to ascend rapidly. Further it can be noticed that in figure 6.7, the terminal voltage has fluctuated during start of the test and this is reflected significantly by rate of change of terminal voltage. Hence the voltage knee point determination solely based on gradient of terminal voltage can project a wrong result.

6.4 Difference of the rate of change of voltage drop to estimate the new knee voltage cut-off point.

Rate of change of terminal voltage itself for deciding the knee point discussed in section 6.3 can be misleading due to the fact that this is subjected to variations due to change of system's loads. Such variations can be miss read as close to knee point situations as shown during first two minutes of the figure 6.8. It shows comparison of rate of change of terminal voltage, during discharging of a good battery(B) with weaker battery (C). The voltage variation during first two minutes of bellow figure 6.8 is clearly an effect of change of load of the system, as the variation has affected both battery B and C. This effect is common to all the batteries in the bank. Hence this same rate of change can be observed in other batteries as well irrespective of whether weak or healthy during load variations.

Hence as an alternative, the difference in the rate of change of terminal voltage between two batteries can be checked to decide the knee point of weak battery/batteries irrespective of the system variations as seen in figure 6.8 where curve $dV_B(t)/dt - dV_C(t)/dt$.

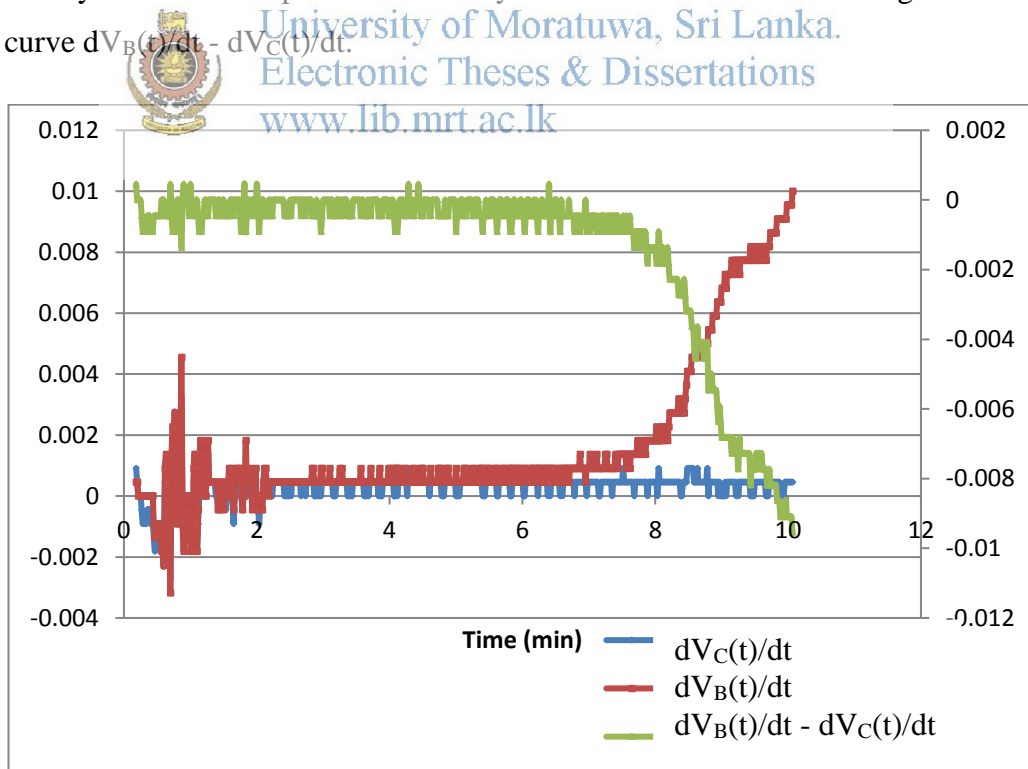


Figure 6.8 : Difference of rate of change of voltage of two batteries near knee point

CONCLUSION.

The modified Thevenin's model based method for estimating the state of charge, can be utilized in an application in the context of batteries in series successfully. Only measured parameters in above technique would be the terminal voltage of individual batteries and current through the whole string. The method largely depend on the linear relationship between SOC and OCV. This data is usually available from the battery manufacturers which needs to be fed for such a controller, which implements the above technique. Alternatively the OCV at two known points(Eg, 30% and 100%) can be measured during initial installation of batteries and this data can be fed to the systems. In addition a calibration test has to be carried annually or when a battery or more in the string is replaced. Though the model fit well in the context of small scale battery installation in a country such as Sri Lanka with almost regular ambient temperature, frequent calibrations would be essential in a different scenario with dramatic ambient changes. It is advantageous that the method does not require to track the start or end points during the regular use of battery installation which can lead to accumulation errors such as Coloumb counting or Peukerts method.

Deciding the battery discharge cut off voltage is crucial parameter for a hybrid inverter based small scale storage with lead acid battery string. A flat discharge voltage cut off point at all stages of the life of battery bank with few weaker batteries can jeopardize the whole storage system. Terminal voltage of weaker battery/batteries start to deviate from others significantly close to its knee point voltage of discharge curve. In chapter 6 it is explained and experimental established that the difference of rate of change of terminal voltage can give a better idea of the weaker battery, thus the discharge cut off point of the whole battery bank without compromising or risking cycle life. There is a great scope of future work for developing an algorithm based on this which can also be applicable for battery parallel configuration.

References

- [1] John Chiasson, Baskar Variamohan, "Estimating the State of Charge of a Battery", Transactions on Control Systems Technology, Vol. 13, NO. 3, May 2005
- [2] James Martin , " Batteries & Energy Storage, Installation Advice, NSW Solar system Products", <http://www.solarchoice.net.au/blog/how-much-energy-storage-capacity-do-you-need>, JANUARY 11, 2016
- [3] Panasonic Sealed Lead-Acid Batteries Technical Handbook 2000.
- [4] Guoliang Wu, Rengui Lu , Chunbo Zhu "Apply a Piece-wise Peukert's Equation with Temperature Correction Factor to NiMH Battery State of Charge Estimation School of Electrical Engineering, Harbin Institute of Technology", Volume 8, Number 2, December 2010
- [5]  <http://www.smartgauge.co.uk/peukert.html>.
University of Moratuwa, Sri Lanka.
Electronic Theses & Dissertations
www.lib.mrt.ac.lk
- [6] Handbook for Gel-VRLA-Batteries.
- [7] <http://www.sciencedirect.com/science/article/pii/S0378775305007093>.
- [8] T. D. O'Sullivan, "Method For Predicting Battery Capacity" US Patent 6211654, April 2001.
- [9] Sealed Lead Acid batteries technical manual
- [10] Christopher Suozzo, B.S.E.E," Lead-Acid Battery Aging And State Of Health Diagnosis" The Ohio State University, 2008.


[11] Phillip E. Pascoe, " Standby VRLA battery reserve life estimation ", Telecommunications Energy Conference, 2004. INTELEC 2004. 26th Annual International, 19-23 Sept. 2004

[12]IEEE Std 450™-2002 IEEE Recommended Practice for Maintenance, Testing, and Replacement of Vented Lead-Acid Batteries for Stationary Applications.

[13] International Renewable Energy Agency (IRENA), "Battery Storage For Renewable: Market Status And Technology Outlook", 2015.

[14] Matthew Barth, Jie Dy, Jay Farrell, Shuo Pang, "Battery state-of-charge estimation", Proceedings of the American Control Conference, Vol. 2, June 2001

[15] Amin Rezaei Pish Robot, "Optimization of Charging Current and SOH Estimation for Lead Acid Batteries", Faculty of Engineering, University of Bonab, Iran, International Journal of Computer Science & Communication Networks, Vol 2(1), 117-122



University of Moratuwa, Sri Lanka
Electronic Theses & Dissertations
www.lib.mrt.ac.lk

[16] Kong Soon Ng ,Chin-Sien Moo, Yi-Ping Chen, Yao-Ching Hsieh, "Enhanced coulomb counting method for estimating state-of-charge and state-of-health of lithium-ion batteries", Applied Energy 86 (2009) 1506–1511